

# Study of The Sorption of The Total Phenolic Compounds From Olive Mill Wastewater By Natural Soils: Conventional and Under Microwave Irradiation Kinetics.

Malika Arabi (✉ [hocinemalikaaa@yahoo.fr](mailto:hocinemalikaaa@yahoo.fr))

Nuclear Research Center <https://orcid.org/0000-0001-5528-0036>

Abdelhamid Elias

Université de Tizi-Ouzou

Yasmine Ait Younes

Algiers Nucleau Research Center

Ziane Kamel

Algiers Nuclear Resarch Center

Idir Toumert

Algiers Nuclear Research Center

Belkacem Mansouri

Algiers Nuclear Research Center

---

## Research Article

**Keywords:** Sorption, conventional, microwave irradiation, total phenolic compounds, olive mill wastewater, natural soils, kinetics and isotherms.

**Posted Date:** November 29th, 2021

**DOI:** <https://doi.org/10.21203/rs.3.rs-1004270/v1>

**License:**  This work is licensed under a Creative Commons Attribution 4.0 International License.

[Read Full License](#)

---

# Abstract

The elimination of total phenolic compounds (TPC) from olive mill wastewater was studied by sorption under the conditions: conventional and under microwave irradiation on previously characterized soils. The sorption process has been studied in batch using inorganic materials in their natural states for sustainable development.

The characterizations of the soils have shown variability in potential of hydrogen (4.6-8.9) in total nitrogen between 0.5 and 2.5% and in mineral matter which varies between 5.86 and 15.16%. On the other hand, the mineralogical characterization showed that the three soils are composed of several clay and non-clay minerals.

The experimental data were analyzed using reaction models and diffusion models. The pseudo second order kinetic model provides the best correlation. It best represents the kinetics of adsorption by the natural adsorbents  $N_1$ ,  $N_3$  and R.

The sorption models of LANGMUIR, FREUNDLICH and DUBININ-RADUSHKEVICH were used for the mathematical description of the conventional adsorption equilibrium. The best correlations were obtained with the model of LANGMUIR ( $r^2 > 0.95$ ) on soils  $N_1$  and  $N_3$  unlike the models of FREUNDLICH and DUBININ-RADUSHKEVICH ( $r^2 < 0.65$ ). The soil R can be represented by the model of FREUNDLICH ( $r^2 \geq 0.96$ ) and the model of LANGMUIR ( $r^2 > 0.93$ ). The latter is confirmed by the value of the dimensionless coefficient  $R_L$ . Removal rates of TPC were calculated. The value obtained (71 %) showed that the soil  $N_1$  is a good adsorbent. The results are satisfactory and promising.

# Introduction

Water is essential for life, but it is also very often at the heart of many economic activities. Oleic vegetation water is industrial wastewater commonly called "vegetable water" and comes from water during the olive oil extraction process (water from the pulp and added water). The quantity produced depends on the demand for olive oil and its extraction procedure which generates with effluents at concentration points pollutants (polyphenols) that cannot be absorbed by the purifying power of the media. They are considered to be one of the most harmful plant discharges by the agro-food industries (Cardinali et al. 2010) due to the toxicity of their pollutant load for the entire ecosystem (plants, microorganisms, aquatic and aerial organisms).

Phenolics, or polyphenols, are secondary metabolites ubiquitous in plants from roots to fruit. They represent organic pollutants very frequently encountered in effluents, coming from waste from olive oil production during winter. They refer to a family of mono or polycyclic aromatic compounds that contribute color and sensory properties such as bitterness and astringency (Dai et al. 2010; Ignat et al. 2011; Ojeil et al. 2010).

Sorption is a very efficient and promising physical separation process used to lower the concentration of toxic organic pollutants in industrial effluents. It is a non-polluting treatment method, easy to apply and has already been proven in the treatment of wastewater (Meçabih et al. 2006; Zidane et al. 2011).

Most Mediterranean countries are currently concerned by the problem of pollution caused by olive oil effluents. The treatment of the latter by adsorption on different solid materials has been the subject of many work to know about on expensive materials such as activated carbon (Aliakbarian et al. 2015; Diamadopoulos et al. 1992; Galiatsatou et al. 2002), activated clays (Al Mallah et al. 2000) and on inexpensive materials such as banana peel (Achak et al. 2009), wheat bran (Achak et al. 2014), ...

The aim of our study is to enhance these natural soils for wastewater treatment by studying their sorption capacities for the removal of TPC.

## Experimental

Materials

### Adsorbats

The adsorbates used in this work come from the olive industry. They were harvested in the region of Tizi-Ouzou in March 2015 from the first olive oil storage basin according to the standard 5667-3 (NI ISO 2012) in dark jerricans of 20 liters in view of their transport to the laboratory for storage at 4°C.

### Adsorbents

The adsorbents (soils) used in this work were collected near the sampling area of our two vegetation waters traditional and modern (Tizi-Ouzou). They are natural and differ from each other in color (red, brown, gray and black). Drying in the open air was preceded before being ground by a porcelain mortar, a sieving at different meshes and storage at room temperature in plastic boxes before characterizations and sorption experiments.

Characterization methods

*Physicochemical characterization*

## 1. Olive mill wastewater (OMWW) characterization

The pH was measured using a pH meter brand WTW multi 340i according to NF T 90-008 (ISO 2001). The electrical conductivity was obtained by means of a conductivity meter of the K 120 CONSORT digital conductivity type according to the French standard NF EN 27888 (1994). The results of the conductivity are expressed in mS/cm at ambient temperature. The TPC, expressed as gallic acid equivalents, were determined by the Folin-Ciocalteu colorimetric method (Box 1983) at the experimental wavelength 765 nm by a UV-visible spectrometer (T60, PG. Instruments), expressed in g/L.

## 2. Soils characterization

The soil pH was determined, according to ISO 10390 (2005), in a soil suspension diluted in water at 1:5 (V/V) and using a Microprocessor pH Meter WTW pH537. For the pH at the zero point charge, its measurement (Babić et al. 1999) consists in placing in a series of Erlenmeyer flasks 40 mL of the KNO<sub>3</sub> solution (10<sup>-1</sup> M, Fluka), previously adjusted to the desired pH varying from 2 to 12 by addition of NaOH or HCl (10<sup>-1</sup> M), in contact with 0.2 g of soil ( $\varphi < 500 \mu\text{m}$ ). The suspensions should be kept under constant stirring at room temperature for 48 h. The final pH is then determined on the supernatant after separation of the two constituents by centrifugation at 3000 g and at 20°C for 15 min. The pH<sub>pzc</sub> is the point of intersection between the curve representing the final pH as a function of the initial pH and the line final pH = initial pH.

Moisture (H) was determined after drying of a mass (m) at 105°C for 24 hours. The rate, expressed as a percentage, was calculated using the formula:

$$H(\%) = (m_0 - m_1/m_0).100 \quad (1)$$

where  $m_0$ ,  $m_1$  are the mass of the sample before and after drying at 105°C expressed in grams, respectively.

Soil densities were measured using a helium pycnometer (Micromeritics) connected to a vacuum system and to a helium cylinder via a pressure regulator (0.3- 0.5 bar). They are calculated by the formula:

$$d_s = \rho_s/\rho_{\text{eau}} = (m_s/(m_L - m_i))/\rho_{\text{eau}} \quad (2)$$

where  $\rho_s$  is the density of the soil,  $\rho_{\text{water}}$  is the density of water at a temperature of 4°C,  $m_s$  is the mass of the soil (Kg),  $m_L$  is the mass of liquid alone (Kg) and  $m_i$  is the mass of the immersion liquid (Kg) in the pycnometer.

The functional groups were identified by Fourier transform infrared spectrometry (NICOLET 380) by preparing potassium bromide KBr (Merck, MM= 119.01 g. mole<sup>-1</sup>) pellets mixed with 1 % of soil powder. The identification of the crystallized mineral species of the soils was carried out by X-ray diffraction (XRD) and this by comparison with a reference file called JCPDS sheets for "Joint Committee for Powder Diffraction Studies" (JCPDS 2000; Mathon 2008). The chemical composition of the soils was determined by the wavelength dispersive X-ray fluorescence technique (WD-XRF). The microstructure of our adsorbents was observed by an FEI Quanta 650 type scanning electron microscope (SEM).

The organic and inorganic matters were determined according to the work of Wang et al. (2012). Organic matter, expressed as a percentage, was calculated using the formula:

$$\text{MOG}(\%) = (m_1 - m_2/m_1).100 \quad (3)$$

where  $m_1$ ,  $m_2$  are the mass of the sample after drying at 105°C and 375°C expressed in grams, respectively.

On the other hand, the mineral material was calculated by the formula:

$$MM(\%) = (m_2 - m_3/m_2).100 \quad (4)$$

where  $m_2$ ,  $m_3$  are the mass of the sample after drying at 105°C and 800°C expressed in grams, respectively.

The loss on ignition was determined after baking at 1000°C of our adsorbent for one hour in a muffle furnace. It is expressed as a percentage and evaluated by the following formula.

$$Pf(\%) = (m_1 - m_4/m_1).100 \quad (5)$$

where  $m_1$ ,  $m_4$  are the mass of the sample after drying at 105°C and 1000°C expressed in grams, respectively.

The cation exchange capacity (CEC) was measured at pH = 9.0 in a sandwich percolation tube between two layers of 10 g of sand (Mathieu, Pieltain 2003).

The specific surface area, also known as mass area, was calculated using the so-called BET (Brunauer et al. 1938) calculation model (Brunauer, Emmett and Teller) at nitrogen at 77°K by a Micromeritics ASAP 2010, USA. The particle size distribution was carried out by sieving using a Retsch type vibrator at vibration amplitude fixed at 40 for 30 minutes.

### Sorption experimental test

The sorption tests for TPC were studied in static mode (batch). The overall experimental parameters chosen to carry out these tests are: time, weight and particle size of the adsorbent, the dilution factor (TPC concentration) and the pH of the effluent. The latter was adjusted to the required pH using either NaOH (1 M) or HCl (1 M). At the end of each sorption study, the adsorbents were separated by centrifugation (SIGMA 3-30 KS) at 3000g for 15 min and at 20°C. Three phases are thus obtained: at the bottom the adsorbent, in the center the olive oil effluent and a very very light layer of oil on the surface.

The content of the TPC was obtained in each case by UV-visible spectrometer at the experimental wavelength 765 nm, after application of the method of Box (1983) on the medium phase, by extrapolation on the calibration curve.

The adsorbed quantity ( $q_e$ ) as well as the removal percentage (R %) of the PC were calculated as a function of the concentration of total phenolic compounds in both wastewaters before and after adsorption per mass unit of soil (0.2 g) and wastewater volume (20 mL) according to the equations, respectively:

$$q_e = (C_0 - C_e).V/w \quad (6)$$

$$R(\%) = (C_0 - C_t).100/C_0 \quad (7)$$

where  $C_0$ ,  $C_e$ , and  $C_t$  are respectively the initial, the equilibrium and at time (t) the phenolic compounds concentrations in the solution during the adsorption process (g/L). V is the volume of the solution (L) and W is the weight of the sorbents (g).

## Conventional sorption test

The experiment was carried out at room temperature and protected from light. For this purpose, 20 mL of non-delipidated oleic effluents were brought into contact with a known weight of each soil separately in open reactors. The suspensions were shaken by a multi-station system (Gesellschaft für Labortechnik mbH, 3015). For each experiment, a control pot was produced under the same conditions without the solid.

## **Under microwave irradiation sorption test**

These microwave irradiation sorption tests were performed in a modified SAMSUNG brand household microwave oven. For this, the natural soils (0.2 g) were placed separately in open reactors (diameter = 4.5 cm; length = 6.8 cm) with 10 mL of olive mill wastewater ( $[OMWW]_0 = 2.652 \text{ g/L}$ ). This mixture (adsorbent-adsorbate) was placed inside a microwave oven and was dispersed by stirring using a glass rod installed in a mechanical stirrer of the IKA RW 20n brand at 250 rpm. The power of the microwave oven was set at 180 W. The microwave irradiation was programmed for a time  $t$  with steps equal to 5 seconds.

*Parametric study of the batch sorption*

### **1. Effect of contact time**

The contact time between the adsorbent (soils) and the adsorbate (TPC) is an important parameter which generally influences the sorption process. It makes it possible to determine the rate of elimination of TPC and therefore to evaluate the effectiveness of the adsorbent. The sorption conditions applied in the conventional method were: 2 g of soil particle size equal to 400  $\mu\text{m}$ , an initial concentration of TPC in OMWW equal to 2.910 g/L. The time was varied from 5 to 420 minutes and the stirring speed was set at 250 rpm. The experimental protocol which was carried out, in a reactor with a capacity of 50 mL, is as follows: 20 mL of diluted olive mill wastewater ( $[TPC] = 0.728 \text{ g/L}$ ) with deionized water are added to 2 g of soil of particle size equal to 400  $\mu\text{m}$ . The solids load in the liquid is  $100 \text{ g} \cdot \text{L}^{-1}$ . Several vials were thus prepared and the suspensions were shaken at room temperature ( $20 \pm 5^\circ\text{C}$ ), at natural effluent and soil pH for variable times ranging from 5 to 420 minutes (contact time per bottle). After stirring, the suspension was thus centrifuged and ready for the determination of the TPC by the protocol of Box (1983).

### **2. Effect of the amount on the sorption capacity of TPC**

This test has been studied in the range 0.5 – 3.5 g with steps of 0.5 g for 24 h to ensure equilibrium. Several flasks were thus shaken, at room temperature ( $20 \pm 5^\circ\text{C}$ ), at 250 rpm at natural effluent pH (4.55) and soil. The particle size of the latter was set at 400  $\mu\text{m}$ . The content of TPC in the effluent, before adsorption, was measured and is equal to 0.728 g/L. After stirring, the suspension was centrifuged and ready for application of the Box assay protocol (1983).

### **3. Effect of the soil particle size of the adsorbent on sorption of TPC**

The effect of soil particle size was studied using different particle sizes ranging from 40 to 400  $\mu\text{m}$  for the three adsorbents and taking into consideration the optimized parameter obtained previously (the previously optimized parameter obtained) such as the mass of the adsorbent (3.5 g). The other operating conditions were set as follows: at 250 rpm for the stirring speed, natural pH of the effluent (4.55) and of the soil, ambient temperature close to 25°C and finally 0.728 mg/L for the content of TPC in the effluent before the application of sorption phenomenon. After stirring, the suspension was centrifuged and ready for application of the Box protocol (1983).

## 4. Effect of pH on sorption capacity of TPC

The influence of pH on the adsorption of TPC by natural soils was studied using the mass (3.5 g) and grain size (40  $\mu\text{m}$ ) optimized in previous experiments. The initial concentration of the olive oil effluent in TPC used is 728 mg/L. The pH values explored range from 3 to 10. The suspensions were stirred at a speed of 250 rpm for a period of time required to reach equilibrium previously determined by the adsorption kinetics study (24 h) at room temperature (20  $\pm$  5°C) and protected from light.

## 5. Effect of the content of t TPC on the sorption capacity

This study consists in following the influence of the initial concentration of the solute on the quantity adsorbed by the adsorbent ranging from the content 5 mg/L up to 189 mg/L and a natural pH of the effluent equal to 4.55. The mass (3.5 g) and the grain size (40  $\mu\text{m}$ ) used are those previously optimized. The suspensions were stirred at a speed equal to 250 rpm for a period of time equal to 24 hours at room temperature (20  $\pm$  5°C) and protected from light.

## 6. Effect of irradiation microwave

The conditions for this effect were set at: a weight equal to 2 g of soil at 40  $\mu\text{m}$ , a power of 180 W, a TPC concentration 663 mg/L, variable times ranging from 5 up to 50 seconds with steps, of 5 seconds, repeated several times in order to avoid boiling (one contact time per flask) and a stirring speed equal to 250 rpm.

## Kinetic studies

The adsorption kinetics makes it possible to estimate the quantity of pollutants adsorbed as a function of time. It provides information on the adsorption mechanism and the transfer mode of solutes from the liquid phase to the solid phase. At equilibrium, the adsorption kinetics of a material can be modeled. For this purpose, the literature reports a number of models that can register as follows:

Pseudo-first order model (Srivastava et al. 2006)

$$\ln(q_e - q_t) = \ln q_e - k_1 \cdot t \quad (8)$$

Pseudo-second order model (Ho and McKay 1999; Li et al. 2008; Martins et al. 2013)

$$t/q_t = (1/k_2 \cdot q_e^2) + (1/q_e) \cdot t \quad (9)$$

Intra-particle-scattering model (Weber and Morris 1963)

$$q_t = k_{int} \cdot t^{1/2} + \alpha \quad (10)$$

Extern scattering model (Al Mardini 2008; Hameed et al. 2008)

$$\ln(1 - (q_t/q_e)) = -0,497 - k_b \cdot t \quad (11)$$

where  $k_1$  ( $\text{min}^{-1}$ ) is the rate constant for the pseudo-first-order model,  $k_2$  ( $\text{g/mg} \cdot \text{min}$ ) is the rate constant for the pseudo-second-order model,  $k_{int}$  ( $\text{mg/g} \cdot \text{min}^{0,5}$ ) is the rate constant for the intra-particle-scattering model,  $k_b$  ( $\text{min}^{-1}$ ) is the rate constant for the extern scattering model,  $q_e$  and  $q_t$  ( $\text{mg/g}$ ) are the amount of solute absorbed per unit adsorbent at equilibrium and at time  $t$ , respectively.  $\alpha$  is the parameter that reflects the deviation of the adsorption process from the intra-particle scattering mechanism.

## Isotherm studies

The equilibrium adsorption isotherms of the solid-liquid system of TPC were determined using the following models:

### 1. LANGMUIR model

The linearization of the equation of the LANGMUIR model is given by the relation:

$$C_e/Q_{eq} = 1/(Q_{max} \cdot K_L) + (1/Q_{max}) C_e \quad (12)$$

where  $Q_e$  and  $Q_{max}$  ( $\text{mg/L}$ ) are the adsorption capacity at equilibrium and maximum of the adsorbent, respectively.  $C_e$  is the equilibrium concentration of TPC in the liquid phase ( $\text{mg/L}$ ) and  $K_L$  is the LANGMUIR equilibrium constant characteristic of the adsorbent ( $\text{L/mg}$ ).

The plot ( $C_e/Q_e$ ) versus  $C_e$  provides a line of slope ( $1/Q_{max}$ ) and intercept ( $1/(Q_{max} \cdot K_L)$ ). The essential characteristics of the LANGMUIR isotherm can be expressed by a dimensionless constant called separation factor or equilibrium parameter " $R_L$ " (Kestioğlu et al. 2005).

$$R_L = 1/(1 + K_L \cdot C_0) \quad (13)$$

The value of this factor indicates the isotherm type: unfavorable if  $R_L > 1$ ; linear if  $R_L = 1$ ; favorable if  $0 < R_L < 1$  or irreversible if  $R_L = 0$ .

### 2. FREUNDLICH model

The linearization of the equation of the FREUNDLICH model is given by the relation:

$$\ln Q_e = \ln K_F + (1/n) \ln C_e \quad (14)$$

This equation is that of a straight line with slope  $1/n$  and intercept  $\ln K_F$ . In general, adsorption is favorable when  $1/n$  is between 2 and 10, moderate for  $1/n$  between 2 and 1, weak for  $1/n$  less than 1 and linear when this constant tends towards 1 (Hamdaoui, Naffrechoux 2007).

where  $Q_e$  and  $Q_{max}$  ( $\text{mg/L}$ ) are the adsorption capacity at equilibrium and maximum of the adsorbent, respectively.  $C_e$  is the equilibrium concentration of TPC in the liquid phase ( $\text{mg/L}$ ) and  $K_f$  and  $1/n$  are the FREUNDLICH constant.

### 3. DUBININ-RADUSHKEVICH (D-R) model

The linearization of the equation of the DUBININ- RADUSHKEVICH model is given by the relation:

$$\ln q_e = \ln q_{\max} - \beta' \cdot R^2 \cdot T^2 (\ln(1 + (1/C_e)))^2 \quad (15)$$

where  $q_{\max}$  is the theoretical saturation capacity (mg/g),  $\beta'$  is a constant related to the adsorption energy ( $\text{mole}^2/\text{kJ}^2$ ),  $R$  is the perfect gas constant ( $8.314 \cdot 10^{-3} \text{ kJ/mole K}$ ),  $T$  is the solution temperature (K) and  $C_e$  is the equilibrium concentration of TPC in the liquid (mg/L).

The constant  $\beta'$  is related to the free energy  $E_D$  by the relation:

$$E_D = 1/\sqrt{2\beta'} \quad (16)$$

The "ED" value to determine the nature of physical or chemical adsorption process. According to the literature (Benhammou et al. 2005; Erhayem et al. 2015):

If :  $E_D < 8 \text{ kJ/mole}$ , the adsorption process is physical;

$E_D$  is between 8 and 16 kJ/mole, the adsorption is an ion exchange process;

$E_D > 16 \text{ kJ/mole}$ , the process is dominated by intra-particle diffusion (*chemical*).

## Results And Discussion

### Olive vegetation water characterization

The main characteristics of the vegetation water used to carry out the adsorption tests are summarized in Table 1. They show that the olive oil discharges are acidic and rich in polluting organic matter.

Table 1  
Main characteristics of olive vegetation water

Parameter	pH	E.C	TPC
Unit	-	mS/cm	g/L
Measured value	4.55	8.61	2.910 ± 0.014
E.C : electrical conductivity; TPC : total phenolic compounds			

### Adsorbents properties

The main chemical properties and composition of the studied soils are given in Table 2. They show that the  $N_3$  soil is acidic (pH = 4.6) which is due to the presence of humic and fulvic substances and to the oxidation of inorganic compounds such as iron sulphide (Kedi 2011; Oertli 2008). The other two soils ( $N_1$  and R) have an alkaline pH of 8.9 and 8.4, respectively. This may be due to the presence of carbonates (Kedi, 2011; Oertli 2008).

Sample N<sub>3</sub> is characterized by a higher total nitrogen content (2.5 %) against 0.85 % for sample N<sub>1</sub> and 0.2 % for soil R.

Mineral matter is present in all three adsorbents. Sample N<sub>1</sub> has the highest content of this material (15.16 %), inorganic carbon (4.14 %) and especially limestone (25.78 %). This last parameter may be at the origin of the alkaline nature of this soil. The greatest value of the loss on ignition is also recorded for sample N<sub>1</sub> (16.55 %), against 13.15 % for sample N<sub>3</sub> and 7.63 % for soil R. These values, considered low for all soils, indicate that the latter are weakly loaded with volatile species.

Table 2  
Physico-chemical characterization of the studied soils

Adsorbent → Parameter ↓	N <sub>1</sub>	N <sub>3</sub>	R
pH (H <sub>2</sub> O)	8.9	4.6	8.4
E.C (dS/m)	0.13	0.04	0.06
d <sup>20</sup> (g/cm <sup>3</sup> )	3.39	2.83	3.14
H (%)	4.25	3.95	4.90
OM (%)	1.822 ± 0.429	2.122 ± 0.113	2.383 ± 0.383
OC (%)	0.911 ± 0.214	1.061 ± 0.057	1.191 ± 0.192
MM (%)	15.159 ± 0.254	10.918 ± 0.371	5.860 ± 0.182
MC (%)	4.137 ± 0.069	2.980 ± 0.101	1.599 ± 0.050
TC (%)	5.048 ± 0.279	4.041 ± 0.151	2.791 ± 0.219
TN (%)	0.85	2.50	0.20
PI (%)	16.547 ± 0.075	13.145 ± 0.675	7.631 ± 0.078
Ss (m <sup>2</sup> /g)	33.181	24.234	37.800
CEC (mg/100 g)	24.54	22.77	24.32
Lime content (%)	25.78	1.87	1.87
E.C: electrical conductivity; d: measured density at 20 °C; H: humidity; TN: Total nitrogen; OM: organic matter; OC: organic carbon; MM: minerals matter; MC: mineral carbon; TC: total carbon; PI: fire loss; Ss: Specific surface; CEC: cation exchange capacity.			

The values of the other characteristics are quite close for all the samples, including the cation exchange capacity (22.77 - 24.54 mg/100 g), the moisture content (3.95 - 4.90 %), the organic matter (1.82 - 2.38 %) and organic carbon (0.91 - 1.19 %) contents. The specific surface area is variable in the three soils (24.234- 37.80 m<sup>2</sup>/g) and remains very low compared to that of clay (700- 800 m<sup>2</sup>/g) (Calvet 2003).

The particle size distribution (Fig. 1) shows that the soils are characterized by a high percentage of the greater fraction than 40  $\mu\text{m}$  (> 97%) for all the studied soils. The lutite fraction (< 40  $\mu\text{m}$ ) is also present, it respectively represents: 0.42, 2.09 and 2.31 % for R, N<sub>3</sub> and N<sub>1</sub> soils.

The physical and chemical characteristics of soils are different. This is shown by the pH values at the zero point charge (pHpzc) of the three soils N<sub>3</sub>, R and N<sub>1</sub> which are respectively: 4.11, 6.39 and 8.17 (Fig. 2).

For the mineralogical composition of each soil type in the raw state (Fig. 3), we can say that it is complex, varied and specific. According to the JCPDS (2000) sheets, it corresponds to different minerals constituting the soils (Table 3).

Each soil is made up of several clay minerals and various other no clay minerals. Some components are found in all the soils studied such as quartz and muscovite. Kaolinite is also present in two soil samples, notably N<sub>1</sub> and R.

The metallic element composition of the three soils was determined by the wavelength dispersive x-ray fluorescence (WD-XRF) technique. It is expressed in oxide equivalent and presented in mass percentages in Table 4.

Table 3  
Mineralogical composition of soils according to X-ray diffractograms

Soil	Clay mineral composition/ formulas	Various mineral composition/ formulas
N <sub>1</sub>	Muscovite ( $KAl_2(AlSi_3O_{10})(OH)_2$ ), Montmorillonite ( $Si_4O_{10}Al_{5/3}Mg_{1/3}Na_{1/3}(OH)_2$ ), Kaolinite ( $Al_2Si_2O_5(OH)_4$ )	Quartz ( $SiO_2$ ), Anatase ( $TiO_2$ ), Calcite ( $CaCO_3$ ), Dolomite ( $CaMg(CO_3)_2$ )
N <sub>3</sub>	Muscovite, Clinochlor ( $Al_2Mg_5Si_3O_{10}(OH)_8$ )	Quartz, Rutile ( $TiO_2$ ), Jarosite ( $K(Fe_3(SO_4)_2(OH)_6$ )
R	Muscovite, Kaolinite, Vermiculite ( $(Mg,Ca)_{0,7}(Mg,Fe,Al)_6$ ( $Al,Si$ ) <sub>8</sub> O <sub>22</sub> (OH) <sub>4</sub> ·8H <sub>2</sub> O	Quartz

The percentages of silica (SiO<sub>2</sub>) and alumina (Al<sub>2</sub>O<sub>3</sub>) are the highest in all soils. These results are in agreement with those of the XRD which revealed the richness of its soils in clay minerals (aluminosilicates) and quartz.

Table 4  
Soils metals oxides composition (mass %)

Adsorbents → Parameters ↓	N <sub>1</sub>	N <sub>3</sub>	R
SiO <sub>2</sub>	42.21 ± 0.10	45.15 ± 0.10	44.84 ± 0.10
Al <sub>2</sub> O <sub>3</sub>	14.57 ± 0.10	23.48 ± 0.10	27.44 ± 0.10
Fe <sub>2</sub> O <sub>3</sub>	5.41 ± 0.07	8.14 ± 0.08	12.34 ± 0.10
CaO	12.42 ± 0.10	0.12 ± 0.01	0.45 ± 0.02
MgO	3.18 ± 0.05	2.48 ± 0.05	1.96 ± 0.04
K <sub>2</sub> O	2.33 ± 0.04	4.76 ± 0.06	1.34 ± 0.03
Na <sub>2</sub> O	0.51 ± 0.02	0.63 ± 0.02	0.29 ± 0.02
MnO	0.040 ± 0.006	0.020 ± 0.004	0.11 ± 0.01
TiO <sub>2</sub>	0.66 ± 0.02	1.24 ± 0.03	1.18 ± 0.03
P <sub>2</sub> O <sub>5</sub>	0.19 ± 0.01	0.31 ± 0.02	0.10 ± 0.01
SO <sub>3</sub>	0.56 ± 0.02	1.64 ± 0.04	0.05 ± 0.06
Total	82.08	87.97	90.1

These soils are also rich in iron; the high value in sample R may explain its red color. The high content of calcium oxide in soil N<sub>1</sub> also confirms the results of the XRD which revealed the presence of calcite only in this sample.

The metals Mg, Mn, Fe, Al and Si, generally constitute the tetrahedral and octahedral layers of clays. Sodium, potassium and calcium are also known as exchangeable cations incorporated into the interfoliar space of clay sheets.

The results of this analysis are in conformity with those of the XRD by confirming the composition, in clays and quartz, of the raw soils studied.

The IRTF spectra of the adsorbents N<sub>1</sub>, N<sub>3</sub> and R, shown in Fig. 4 reveal the vibration bands of the bonds constituting the minerals that make the studied soils.

The main vibration bands of the bonds (Böke et al. 2004; Ding et al. 2002; Filip and Demnerova 2007; Handke and Mozgawa 1993; Lee et al. 2018; Madejová 2003; Maglione and Carn 1975; Marinovic´ et al. 2011; Ndzana 2018; Reig 2002; Saikia and Parthasarathy 2010; Saikia et al. 2003; Trezza and Lavat

2001; Van der Marel and Beutelspacher 1977) which characterize the minerals present in the studied soils are grouped together in Table 5.

Table 5  
IRTF spectra interpretation of the studied soils

Soils and wave number corresponding to the vibration bands (cm <sup>-1</sup> )			Vibration type
N <sub>1</sub>	N <sub>3</sub>	R	
3619.732	*	3619.732	Elongations of O-H structural bonds
3426.885	*	3426.885	Elongations of O-H bonds in H <sub>2</sub> O hygroscopic
1623.769	*	*	Deformation of O-H bands in water molecules
1428.994	*	*	C-O calcite vibration
1095.369; 1035.587	1095.369; 1022.087	1095.369; 1022.087	Si-O valence vibration in clays
914.09	914.02	914.09	Deformation AlAlOH
875.5	*	*	Vibration of the C-O bond of Calcite
796.457	*	*	Vibrations of Quartz Si-O bonds
711.604	*	*	
694.248	*	*	Vibration of OH deformation
522.614	522.614	522.614	Vibrations of Si-O
470.545	470.546	470.546	Si-O bonds of Quartz
The sign * indicates that the band is not observed in the IR spectrum of the corresponding soil.			

These results show that the vibration bands observed correspond well to those of aluminosilicate minerals links which generally make up clays. These links are: Si-O, O-H, Al-O-H which are found, in particular in montmorillonite, muscovite, kaolinite, vermiculite, clinoclhor and quartz. This further confirms that these minerals make up the studied soils and thus joins the results revealed by XRD and WD-XRF.

Observations with a scanning electron microscope show that the adsorbents N<sub>1</sub> and N<sub>3</sub> appear to have a more porous surface than the third adsorbent R which appears with a rough image (Fig. 5). The grain size ranges between 0.89 and 5.559 µm.

The EDX analysis perfectly confirms the results obtained by the mineralogical and chemical analyzes. It demonstrates the intensity of the calcium peak, characteristic of carbonates which appears very high only in soil N<sub>1</sub> (Fig. 6a). The high calcium content in soil N<sub>1</sub> is also confirmed by the results of other analyzes, including: XRD and X-ray fluorescence.

The EDAX spectra also reveal the presence of silicates, characteristic of quartz and clays that make up the three soils.

It is important to note, according to the EDAX spectra, that the chemical composition of the soils is predominated by the elements: Si, Al and Fe with in addition the element S for the soil N<sub>3</sub> and Ca, Mg for the soil N<sub>1</sub> which contains calcite and dolomite based on XRD analyzes.

The EDAX spectra also reveal the presence of other low intensity peaks, reflecting the presence of other elements with lower contents, namely: phosphorus, sulfur, titanium in soil N<sub>1</sub>; calcium in soil N<sub>3</sub>; potassium, calcium and titanium in soil R.

Sorption studies

## Effects of contact time

These curves show two phases and show that the time to reach almost adsorption equilibrium is about 2 h for the N<sub>1</sub> soil and 4 h for the N<sub>3</sub> and R soils (Fig. 7). The first phase, during which adsorption of almost of the TPC occurs, is characterized by a relatively short duration (1 h) and a rapid adsorption rate. In the second phase, which ends in equilibrium, the adsorption rate and the adsorbed amount are low. The adsorption is faster in the case of soil N<sub>1</sub> and the adsorption capacity of the latter, at equilibrium, is the highest (70.1 %); it is double that of soil R (45.5 %). This can be explained by the low porosity of the soil R (see SEM image).

By comparing our results with those of the literature, we deduce that the adsorption process of PC on our adsorbents is also slow and agrees with the results (2- 12 hours) of many studies (Achak et al. 2009, 2014; Biglari et al. 2016; Buran et al. 2014; Chaudhary and Balomajumder 2014; Djebbar et al. 2012; Kannam and Krauppasmy 1998; Karbowski et al. 2010; Singh et al. 1994; Thawornchaisit and Pakulanon 2007), like those carried out on clay minerals (bentonites) originating from Maghnia (Algeria).

However, according to some studies, the kinetics can be much faster in the cases of some activated adsorbents, such as the adsorption of phenol to activated carbon (Qadeer and Rehan 2002) and on some activated clays (El Gaidoumi et al. 2015). The contact time chosen for the rest of our studies is 24 hours to ensure that equilibrium is reached for the three adsorbents N<sub>1</sub>, N<sub>3</sub> and R.

## Effects of amount on the adsorption capacity of TPC

The results show that when removing TPC by adsorption on natural soils, the rate of removal of TPC increases with the weight of adsorbent used (Fig. 8). It reaches 69, 70 and 73 %, respectively on soils N<sub>3</sub>,

N<sub>1</sub> and R. According to the work of Garg et al. (2004), the increase in adsorption percentage with soil mass may be due to the increase in adsorbent area and adsorption sites (Aarfane et al. 2014; Uddin et al. 2007). The best removal rate is obtained for weights ranging from 3 to 4 g for all soils.

## **Effects of the soil particle size of the adsorbent on adsorption of TPC**

The results show that the increase in particle size make (Fig. 9) decreases the adsorption capacity of TPC due to the decrease in the specific surface area, so the adsorption capacity. The best removal rate is obtained for the fine fractions ( $\varphi = 40 \mu\text{m}$ ).

## **Effects of effluent pH on adsorption capacity of TPC**

The effect of pH on the adsorption capacity of TPC from the effluent by natural adsorbents (N<sub>1</sub>, N<sub>3</sub> and R) shows that the adsorption of TPC is largely affected by the pH of the solution (Fig. 10). The adsorption capacity of TPC in an acidic solution is important for all soils. It is maximum around the pH of the effluent (4.55) for the adsorbents named N<sub>3</sub> (88.8 %) and N<sub>1</sub> (70.8 %). For soil R, the adsorption capacity (78.4 %) is almost constant over the entire pH range.

Comparable results were also found in certain studies on the adsorption of phenols such as those published by: Djebbar et al. (2012) on clays and by Datta et al. (2011) on an ion exchange resin.

## **Effects of the initial content of TPC on the adsorption capacity**

The adsorption capacities of TPC increase with the initial concentration of the latter until the saturation of the adsorption sites, indicated by a plateau (Fig. 11). The maximum adsorbed quantity  $Q_{\text{max}}$  is approximately 0.1 mg of PC/g of adsorbent, or exactly: 0.098; 0.103 and 0.108 mg/g for N<sub>3</sub>, N<sub>1</sub> and R, respectively. It is reached from the initial TPC concentration of 45.5 mg/L.

### *Effect of irradiation microwave*

#### *1. Temperature at the end reaction of microwave irradiation*

The temperatures at the end of the reaction of the adsorbents studied are variable (Fig. 12). It varies between 36.81°C (soil N<sub>3</sub>) and 33.10°C (soil N<sub>1</sub>).

#### *2. Effect of the contact time*

Analysis of the curves (Fig. 13) shows that the rate of adsorption of TPC by the three adsorbents (N<sub>1</sub>, N<sub>3</sub> and R) changes rapidly until it reaches saturation. We can say that microwave irradiations generate the very rapid rotation of molecules. As a result, it creates instantaneous heating of the medium and additional shock movement between molecules, which increases the probability of interaction and the speed of reactions.

The retention by the adsorbent R is faster than in the case of other adsorbents  $N_1$  then  $N_3$ . This difference in adsorption retention comes from the specific surface area of soil R which is relatively greater (37.8  $m^2/g$ ) than those of other soils  $N_1$  (33.18  $m^2/g$ ) and  $N_3$  (24.23  $m^2/g$ ).

Indeed, according to the literature, microwave irradiations accelerate reaction speeds and increase adsorption capacity [Foo et al. 2009] while preserving the pore structure and active adsorption sites [Foo et al. 2012].

By comparing our results with similar work in the literature (Table 6, Fig. 7, Fig. 13: effect of contact time on the adsorption of TPC), we notice that our soil samples are effective in removing the total phenolic compounds in aqueous solutions under the effect of microwave irradiation. Finally, the use of microwave activation reduced the time required to reach equilibrium.

Table 6  
Comparison of the amount of phenol adsorbed by different adsorbents

Author's	Adsorbent		Maximum sorption capacity
Arellano-Cárdenas et al. (2005)	Hétéro-structure d'argile poreuse		14.5 mg/g
Chen et al. (2011)	Argile solidifiée		8.4 mg/g
Chaudhary et al. (2014)	Cendres volantes imprégnées d'aluminium		12.67 mg/g
This work	Natural soil $N_1$	Conventional sorption	2.67 mg/g
		Sorption under microwave activation	10.63 mg/g
	Natural soil $N_3$	Conventional sorption	2.49 mg/g
		Sorption under microwave activation	8.82 mg/g
	Natural soil R	Conventional sorption	1.66 mg/g
		Sorption under microwave activation	19.76 mg/g

### Sorption kinetic

The plots of the sorptions kinetics of the TPC (Fig. 14 and 15) show that the pseudo-second order model is suitable for describing the adsorption reactions of the TPC by the three soils ( $N_1$ ,  $N_3$  and R) for the two processes because the determination coefficients are much closer to unity, so this model describes the

empirical results well. The kinetic parameters ( $k_2$ ,  $q_e$  and  $r^2$ ) deduced from the applied kinetic models are summarized in Table 7.

The coefficients of determination  $r^2$  obtained for the pseudo-second order model are equal in decreasing order to 1.000; 0.975 and 0.971 on soils named respectively  $N_1$ , R and  $N_3$  for the conventional adsorption and 0.99 for adsorption under microwave irradiation.

Table 7  
Kinetic parameters calculated from the models studied for sorption of TPC in olive waste water on the three adsorbents

Adsorbents →		$N_1$ →		$N_3$		R	
		Conv.	μ.wave	Conv.	μ.wave	Conv.	μ.wave
Sorption processes →		Conv.	μ.wave	Conv.	μ.wave	Conv.	μ.wave
↓ Kinetic models							
Pseudo- first order	$k_1$ ( $min^{-1}$ )	0.022	0.044	0.027	0.065	0.021	0.119
	$Q_{max}$ ( $mg/g$ )	0.693	0.118	2.793	1.605	1.684	9.836
	$r^2$	0.201	-0.070	0.264	0.016	0.214	0.114
Pseudo- second order	$k_2$ ( $g/mg\ min$ )	0.211	12.423 $10^{-5}$	1.479	244.344 $10^{-5}$	8.923	0.766 $10^{-5}$
	$q_e$ ( $mg/g$ )	2.669	10.807	2.583	8.752	1.867	20.602
	$r^2$	1.000	0.991	0.971	0.993	0.975	0.991
Intra-particle scattering	$k_{int}$ ( $mg/g\ min^{0.5}$ )	0.068	1.033	0.106	1.049	0.087	2.081
	$\chi$	1.571	5.135	0.674	2.455	0.082	9.187
	$r^2$	0.389	0.383	0.689	0.701	0.934	0.450
Extern scattering	$k_b$ ( $min^{-1}$ )	0.025	0.072	0.025	0.099	0.019	0.113
	$r^2$	0.475	0.283	0.429	0.534	0.377	0.585
Conv. : Conventional; μ.wave : microwave.							

The values of the adsorbed quantities  $Q_e$  calculated by this model are very close to the experimental values for the two sorption processes conventional and under microwave activation (Table 8). This shows that the adsorptions kinetics are perfectly described by the pseudo-second order kinetic model for the three adsorbents chosen to conduct this study.

Similar results were observed for the adsorption of phenolic compounds by banana peel, wheat bran and by activated carbon (Achak et al. 2014; Aliakbarian et al. 2015; Thawornchaisit and Pakulanon 2007). Also, Silva et al. (2012) have shown that the sorption of aromatic compounds on clay supports obeys the pseudo-second order kinetic model.

According to Ho and McKay (2000), the adsorption is of the chemisorption type with the involvement of valence forces by sharing or exchange of electrons between the adsorbent and the adsorbate.

Table 8  
Adsorption amounts of TPC

	$Q_e$ (mg/g)					
	Conventional sorption			Under microwave activation sorption		
Soils	$N_1$	$N_3$	R	$N_1$	$N_3$	R
Experimental values	2.671	2.485	1.657	11.689	8.820	21.979
Measured values	2,669	2,583	1,867	10,807	8,752	20,602

### Sorption isotherm

The sorption isotherms of the TPC on the three natural soils show a classic type L appearance, subgroup 1 for soils  $N_1$ ,  $N_3$  and subgroup 2 for soil R. The plots obtained are illustrated in Fig. 16.

The maximum amount adsorbed at equilibrium  $Q_{max}$  is approximately 0.1 mg of TPC/ g of adsorbent, or exactly: 0.098, 0.103 and 0.108 mg/g for  $N_3$ ,  $N_1$  and R, respectively. These amounts correspond to equilibriums concentrations of TPC of 22.5 mg/L for  $N_1$  and  $N_3$  soils and 20 mg/L for R soil. These results show that the equilibriums concentrations of TPC in the aqueous phase and in the three adsorbents are close.

The models of these adsorption isotherms, illustrated in their linear forms, are illustrated by the plots in Fig. 17, 18 and 19. The parameters obtained from these models ( $K_F$ ,  $1/n$ ,  $Q_{max}$ ,  $K_L$ ,  $\beta$ ,  $E_D$  and  $r^2$ ) for the conventional adsorption of TPC on the three natural soils are determined graphically and listed in Table 9.

According to the values of the determination coefficient  $r^2$ , it is found that the Langmuir model gives a good representation of the adsorption of TPC 0.957 ( $N_1$ ); 0.972 ( $N_3$ ) and 0.936 (R). The dimensionless separation factor  $R_L$  confirms that this isotherm is favorable because its measured value is between zero and one. Namely that the Langmuir model is established on the following assumptions: the equivalence of all the adsorption sites, the non-dependence of the adsorption energy with the coverage rate of the surface, the absence of interactions between the adsorbed and adjacent species on the surface, the

reversibility of the adsorption, which is therefore essentially physical, and the uniformity of the surface of the solid.

**Table 9** Parametric values of the models chosen for this study for the conventional adsorption of TPC from the modern vegetable water studied on the three adsorbents

Adsorbents →		N <sub>1</sub>	N <sub>3</sub>	R	
↓ Isotherms					
	Freundlich	$K_F (L/mg)$	$7.702 \cdot 10^{-6}$	$12.354 \cdot 10^{-6}$	$10.451 \cdot 10^{-6}$
		$1/n$	1.011	0.802	0.891
		$R^2$	0.644	0.453	0.957
Langmuir					
		$K_L (L/mg)$	0.058	0.088	0.067
		$Q_{max} (mg/g)$	0.180	0.140	0.190
		$R_L$	0.105	0.072	0.093
	$R^2$	0.957	0.972	0.936	
Dubinin-Radushkevich					
		$q_{max} (mg/g)$	$10.696 \cdot 10^{-5}$	$9.847 \cdot 10^{-5}$	$10.667 \cdot 10^{-5}$
		$\beta (mole/kJ)^2$	1.854	1.164	1.375
		$E_D (kJ/mole)$	0.519	0.655	0.603
	$R^2$	0.385	0.298	0.464	

However, the Freundlich isotherm provided a better match for the adsorption of TPC to soil R because the value of the determination coefficient  $r^2$  is closest to unity (0.957). The classification of these isotherms (L) confirms the slowness of the process because the attractions forces between the adsorbed molecules are weak.

## Conclusion

The objective of this study was to find the optimal conditions for the elimination of TPC from olive mill wastewater. Our experimental tests were aimed at testing the adsorption power of natural soils under conventional and microwave conditions. They were chosen in order to reduce costs and simplify the process of treating of olive waste water.

The results showed that the retention of the TPC is faster under the conditions under microwave irradiation than under the conventional conditions. Equilibrium is reached after 5-10 seconds unlike

conventional sorption where the shortest equilibrium time is 2 hours.

The results of the kinetic study for all the pollutants show that the retention is very rapid under the conditions under microwave irradiation, it is almost instantaneous. The linear regressions have shown that the kinetics are controlled by the pseudo-second order model. This is clearly confirmed by the values of determination coefficients corresponding to each model.

The study of the sorption isotherm has shown that the experimental data are well reproduced by the Langmuir model for the adsorbents N<sub>1</sub>, N<sub>3</sub> ( $r^2 > 0.95$ ) and by the Freundlich model for the adsorbent R ( $r^2 \geq 0.96$ ). The Langmuir model can also be described on the soil R because  $r^2 = 0.94$ . The dimensionless separation factor ( $R_L$ ) confirms the application of this last model since it is between zero and one, therefore favorable.

In view of these results, it is concluded that the conventional sorption process is slow and better compared to the sorption under the effect of microwave irradiation which is more than fast. The TPC removal rate is acceptable under conventional conditions because it reaches 71 % on soil N<sub>1</sub>. The removal of TPC by conventional sorption is better than sorption under microwave irradiation.

## Declarations

### Acknowledgements

The authors are extremely grateful to Mr. TOUKAL R, former Secretary General and former Director General of the CRNA, for having facilitated all the administrative and logistical aspects (products, small laboratory equipment, etc.) linked to the performance of this work; and this during his terms of office.

On behalf of the co-authors, I herewith testify that the contents of the manuscript, entitled " Study of the sorption of the total phenolic compounds from olive mill wastewater by natural soils: conventional and under microwave irradiation kinetics", are original and have never been published or submitted elsewhere.

- Ethics approval and consent to participate

Not applicable.

- Consent for publication

Not applicable.

- Availability of data and materials

Not applicable.

- Competing interests

The authors declare that they have no competing interests.

- Funding

The authors have no financial or proprietary interests in any material discussed in this article.

- Author's contributions

All the authors contributed to the realization of this work in a complementary way. The methodology as well as the writing of the article was carried out by ARABI M; the sampling of olive mill wastewater, the application of the adsorption process (conventional and under microwave irradiation) as well as the application of the TPC measurement protocol and the optical density readings by UV-visible were carried out by ARABI M and AIT YOUNES Y, the adsorbents were collected by ELIAS A, the characterization of the adsorbents was carried out by ARABI M, ZIANE K, TOUMERT I and MANSOURI B. This manuscript is the work of a whole research team which approves the valuation of the results found.

## References

1. Aarfane A, Salhi A, El Krati M, Tahiri S, Monkade M, Lhadi EK, Bensitel M (2014) Etude cinétique et thermodynamique de l'adsorption des colorants Red195 et Bleu de méthylène en milieu aqueux sur les cendres volantes et les mâchefers. *J Mater Environ Sci* 5:1927–1939
2. Achak M, Hafidi A, Mandi L, Ouazzani N (2014) Removal of phenolic compounds from olive mill wastewater by adsorption onto wheat bran. *Desalination Water Treat* 52:2875–2885. DOI: 10.1080/19443994.2013.819166
3. Achak M, Hafidi A, Ouazzani N, Sayadi S, Mandi L (2009) Low cost biosorbent “banana peel” for the removal of phenolic compounds from olive mill wastewater: Kinetic and equilibrium studies. *Journal of Hazardous Materials* 166:117–125. DOI: 10.1016/j.jhazmat.2008.11.036
4. Al Mallah K, Asma OJ, Abu Lail NI (2000) Olive mills effluent (OME) wastewater post-treatment using activated clay. *Sep Purif Technol* 20:225–234. DOI: 10.1016/S1383-5866(00)00114-3
5. Al Mardini F (2008) Etude de l'adsorption du pesticide Bromacil sur charbon actif en poudre en milieu aqueux- Effet compétiteur des matières organiques naturelles. Dissertation, University of Poitiers
6. Aliakbarian B, Casazza AA, Perego P (2015) Kinetic and Isotherm Modelling of the Adsorption of Phenolic Compounds from Olive Mill Wastewater onto Activated Carbon. *Food Technol Biotechnol* 53:207–214. DOI: 10.17113/ft b.53.02.15.3790
7. Arellano-Cárdenas S, Gallardo-Velázquez T, Osorio-Revilla G, López-Cortéz MS, Gómez-Perea B (2005) Adsorption of phenol and dichlorophenols from aqueous solutions by porous clay heterostructure (PCH). *J Mex Chem Soc* 49:287–291
8. Babić BM, Milonjić SK, Polovina MJ, Kaludierović BV (1999) Point of zero charge and intrinsic equilibrium constants of activated carbon cloth. *Carbon* 37:477–481

9. Benhammou A, Yaacoubi A, Tanouti B (2005) Study of mercury (II) and chromium (VI) adsorption from aqueous solution by Moroccan stevensite. *Journal of Hazardous Materials* 117:243–249
10. Biglari H, Afsharnia M, Javan N, Sajadi SA (2016) Phenol removal from aqueous solutions by adsorption on activated carbon of miswak's root treated with  $\text{KMnO}_4$ . *Iranian Journal of Health Sciences* 4:20–30. DOI: 10.18869/acadpub.jhs.4.1.20
11. Böke H, Akkurt S, Özdemir S, Göktürk EH, Saltik ENC (2004) Quantification of  $\text{CaCO}_3$ – $\text{CaSO}_3$   $0.5\text{H}_2\text{O}$ – $\text{CaSO}_4$   $2\text{H}_2\text{O}$  mixtures by FTIR analysis and its ANN model. *Mater Lett* 58:723–726
12. Box JD (1983) Investigation of the Folin–Ciocalteu phenol reagent for the determination of polyphenolic substances in natural waters. *Water Res* 17:511–525
13. Brunauer S, Emmet PH, Teller E (1938) The use of low temperature Van der Waals adsorption isotherm in determining surface area. *J Amer Chem Soc* 60:309–317
14. Buran TJ, Sandhu AK, Li Z, Rock CR, Yang WW, Gu L (2014) Adsorption/desorption characteristics and separation of anthocyanins and polyphenols from blueberries using macroporous adsorbent resins. *J Food Eng* 128:167–173. DOI: 10.1016/j.jfoodeng.2013.12.029
15. Calvet R (2003) *Le sol, propriétés et fonctions. Tome 1: Constitution et structure, phénomènes aux interfaces.* Dunod, Paris
16. Cardinali A, Cicco N, Linsalata V, Minervini F, Pati S, Peralice M, Tursi N, Lattanzio V (2010) Biological Activity of High Molecular Weight Phenolics from Olive Mill Wastewater. *J Agric Food Chem* 58:8585–8590. DOI: 10.1021/jf101437c
17. Chaudhary N, Balomajumder C (2014) Optimization study of adsorption parameters for removal of phenol on aluminum impregnated fly ash using response surface methodology. *J Taiwan Inst Chem Eng* 45:852–859
18. Chen Y, Ye W, Zhang K (2011) Factors affecting phenol adsorption on clay-solidified grouting curtain. *J Cent South Univ Technol* 18:854–858. DOI: 10.1007/s11771-011-0773-8
19. Dai J, Mumper RJ (2010) Plant Phenolics: Extraction, Analysis and Their Antioxidant and Anticancer Properties. *Molecules* 15:7313–7352. DOI: 10.3390/molecules15107313
20. Datta C, Dutta A, Dutta D, Chaudhuri S (2011) Adsorption of polyphenols from ginger rhizomes on an anion exchange resin Amberlite IR-400 – Study on effect of pH and temperature. *Procedia Food Sci* 1:893–899. DOI: 10.1016/j.profoo.2011.09.135
21. Diamadopoulos E, Samaras P, Sakellaropoulos GP (1992) The effect of activated carbon properties on the adsorption of toxic substances. *Wat Sci Tech* 25:153–160
22. Ding G, Novak JM, Amarasiriwardena D, Hunt PG, Xing B (2002) Soil Organic Matter Characteristics as Affected by Tillage Management. *SOIL SCI SOC AM J* 66:421–429
23. Djebbar M, Djafri F, Boucekara M, Djafri A (2012) Adsorption of phenol on natural clay. *Appl Water Sci* 2:77–86. DOI: 10.1007/s13201-012-0031-8
24. El Gaidoumi A, Chaouni Benabdallah A, Lahrichi A, Kherbeche A (2015) Adsorption du phénol en milieu aqueux par une pyrophyllite Marocaine brute et traitée. *J Mater Environ Sci* 6:2247–2259

25. Erhayem M, Al-Tohami F, Mohamed R, Ahmida K (2015) Isotherm, Kinetic and Thermodynamic Studies for the Sorption of Mercury (II) onto Activated Carbon from Rosmarinus officinalis Leaves. *American Journal of Analytical Chemistry* 6:1–10. <http://dx.doi.org/10.4236/ajac.2015.61001>
26. Filip Z, Demnerova K (2007) Humic substances as a natural factor lowering ecological risk in estuaries. I. Linkov (Eds.), *Environmental Security in Harbors and Coastal Areas*, pp 343–353
27. Foo KY, Hameed BH (2009) Recent developments in the preparation and regeneration of activated carbons by microwaves. *Adv Colloid Interface Sci* 149:19–27. DOI: 10.1016/j.cis.2008.12.005
28. Foo KY, Hameed BH (2012) Microwave-assisted regeneration of activated carbon. *Bioresour Technol* 119:234–240. DOI: 10.1016/j.biortech.2012.05.061
29. Galiatsatou P, Metaxas M, Arapoglou D, Kasselouri-Rigopoulou V (2002) Treatment of olive mill waste water with activated carbons from agricultural by-products. *Waste Manag* 22:803–812. DOI: 10.1016/S0956-053X(02)00055-7
30. Garg VK, Kumar R, Gupta R (2004) Removal of malachite green dye from aqueous solution by adsorption using agro-industry waste: a case study of *Prosopis cineraria*. *Dyes Pigm* 62:1–10
31. Hamdaoui O, Naffrechoux E (2007) Modeling of adsorption isotherms of phenol and chlorophenols onto granular activated carbon. Part I. Two-parameter models and equations allowing determination of thermodynamic parameters. *J Hazard Mater* 147:381–394. DOI: 10.1016/j.jhazmat.2007.01.021
32. Hameed BH, Tan IAW, Ahmad AL (2008) Adsorption isotherm, kinetic modeling and mechanism of 2,4,6-trichlorophenol on coconut husk-based activated carbon. *Chem Eng J* 144:235–244. DOI: 10.1016/j.cej.2008.01.028
33. Handke M, Mozgawa W (1993) Vibrational spectroscopy of the amorphous silicates. *Vib Spectrosc* 5:75–84
34. Ho YS, MCKay G (1999) Pseudo-second order model for sorption processes. *Proc Biochem* 34:451–465
35. Ho YS, MCKay G (2000) The kinetics of sorption of divalent metal ions onto sphagnum moss peat. *Wat Res* 34:735–742
36. Ignat I, Volf I, Popa VI (2011) A critical review of methods for characterisation of polyphenolic compounds in fruits and vegetables. *Food Chem* 126:1821–1835. DOI: 10.1016/j.foodchem.2010.12.026
37. JCPDS, PCPDwin (2000) Diffraction data CD-ROM. Ed. of the International Centre of Diffraction Data. Newtown Square P.A
38. Kannam N, Krauppasmy K (1998) Low cost adsorbents for removal of phenolic acid from aqueous solution. *Ind. J. Env. Prot.* 18:683-697. In: Numbonui Ghogomu J, Tsemo Noufame D, Buleng Njoyim Tamungang A, Ajifack DL, Nsami NDI J and Mbadcam Ketcha J (2014) Adsorption of phenol from aqueous solutions onto natural and thermally-modified kaolinitic materials. *Int J Biol Chem Sci* 8:2325-2338
39. Karbowski T, Mansfield AK, Barrera-García VD, Chassagne D (2010) Sorption and diffusion properties of volatile phenols into cork. *Food Chem* 122:1069–1094

40. Kedi ABB (2011) Fonctionnement des phosphatases dans les sols tropicaux: Influence de la composition organo-minérale sur l'expression de l'activité enzymatique. Dissertation, Montpellier SupAgro; Co-supervised with the University of Cocody- Abidjan UFR Structural Sciences of Matter and Technology (SSMT)
41. Kestioğlu K, Yonar T, Azbar N (2005) Feasibility of physico-chemical treatment and Advanced Oxidation Processes (AOPs) as a means of pretreatment of olive mill effluent (OME). *Process Biochem* 40:2409–2416
42. Lee BS, Lin HP, Chan JCC, Wang WC, Hung PH, Tsai YH, Lee YL (2018) A novel sol-gel-derived calcium silicate cement with short setting time for application in endodontic repair of perforations. *Int J Nanomed* 13:261–271
43. Li W, Zhang L, Peng J, Li N, Zhang S, Guo S (2008) Tobacco Stems as a Low Cost Adsorbent for the Removal of Pb(II) from Wastewater: Equilibrium and Kinetic Studies. *Ind Crops Prod* 28:294–302
44. Madejová J (2003) FTIR techniques in clay mineral studies. *Vib Spectrosc* 31:1–10. DOI: 10.1016/S0924-2031(02)00065-6
45. Maglione G, et Carn M (1975) Spectres infrarouges des minéraux salins et des silicates néoformes dans le bassin Tchadien. *Cah ORSTOM, sér. Géol., Vol.VII.* 1:3-9
46. Marinović S, Vuković Z, Nastasović A, Milutinović-Nikolić A, Jovanović D (2011) Poly(glycidyl methacrylate-co-ethylene glycol dimethacrylate)/clay composites. *Materials Chemistry and Physics* 128:291-297. DOI: 10.1016/j.matchemphys.2011.03.018. In: Awaleh MO, Farah IG, Adawe LF, Egueh NM, Soubaneh YD, Caminiti AM, Hoch FB, Etoubleau J (2014) Potentialite d'utilisation d'argiles Djiboutiennes dans l'industrie céramique. ScienceLib Editions Mersenne. 6, N°141106, ISSN 2111-4706
47. Martins AE, Pereira MS, Jorgetto AO, Martines MAU, Silva RIV, Saeki MJ, Castro GR (2013) The reactive surface of Castor leaf (*Ricinus communis* L.) powder as a green adsorbent for the removal of heavy metals from natural river water. *Appl Surf Sci* 276:24–30. DOI: 10.1016/j.apsusc.2013.02.096
48. Mathieu C, Pieltain F (2003) Analyse chimique des sols: méthodes choisies. TEC & DOC éd. LAVOISIER. ISBN: 2-7430-0620-X
49. Mathon M-H (2008) Caractérisation des textures par diffraction neutronique. *Collection SFN* 9:49–64
50. Meçabih Z, Kacimi S, Bouchikhi B (2006) Adsorption des matières organiques des eaux usées urbaines sur la bentonite modifiée par Fe(III), Al(III) et Cu(III). *Revue des Sciences de l'Eau* 19:23–31. <https://doi.org/10.7202/012261ar>
51. Ndzana GM, Huang L, Wang JB, Zhang ZY (2018) Characteristics of clay minerals in soil particles from an argillic horizon of Alfisol in central China. *Appl Clay Sci* 151:148–156. DOI: 10.1016/j.clay.2017.10.014
52. NF EN 27888 (1994) Qualité de l'eau- Détermination de la conductivité électrique
53. NF ISO 10390 (2005) Qualité du sol- Détermination du pH
54. NF T 90-008 (2001) Qualité de l'eau- Détermination du pH

55. NI ISO 5667-3 (2012) Qualité de l'eau- Echantillonnage. Partie 03: Conservation et manipulation des échantillons d'eau
56. Oertli JJ (2008) Soil fertility, In: Chesworth W éd., Encyclopedia of soil science. Springer-Verlag GmbH, Heidelberg Germany, pp 656-668
57. Ojeil A, El Darra N, El Hajj Y, Bou Mouncef P, Rizk TJ, Maroun RG (2010) Identification et caractérisation de composés phénoliques extraits du raisin château ksara. Lebanese Science Journal 11:117–131
58. Qadeer R, Rehan AH (2002) A study of the adsorption of phenol on activated carbon from aqueous solutions. Tur J Chem 26:357–361
59. Reig FB, Gimeno Adelantado JV, Moya Moreno MCM (2002) FTIR Quantitative analysis of calcium carbonate (calcite) and silica (quartz) mixtures using the constant ratio method. Application to geological samples. Talanta 58:811–821. PMID: 18968811.
60. Saikia BJ, Parthasarathy G (2010) Fourier Transform Infrared Spectroscopic Characterization of Kaolinite from Assam and Meghalaya, Northeastern India. J Mod Phys 1:206–210. DOI: 10.4236/jmp.2010.14031
61. Saikia NJ, Bharali DJ, Sengupta P, Bordoloi D, Goswamee RL, Saikia PC, Borthakur PC (2003) Characterization, beneficiation and utilization of a kaolinite clay from Assam, India. Appl Clay Sci 24:93–103
62. Silva MMF, Oliveira MM, Avelino MC, Fonseca MG, Almeida RKS, Silva Filho EC (2012) Adsorption of an industrial anionic dye by modified-KSF-montmorillonite: Evaluation of the kinetic, thermodynamic and equilibrium data. Chem Eng J 203:259–268
63. Singh B, Mish N, Rawat N (1994) Sorption characteristic of Phenols on fly ash and impregnated fly ash. Ind J Env Hlth 38:1–14
64. Srivastava VC, Swamy MM, Malli D, Prasad B, et Mishra IM (2006) Adsorptive removal of phenol by bagasse fly ash and activated carbon: Equilibrium, kinetics and thermodynamics. Colloids Surfaces A: Physicochem Eng Aspects 272:89–104
65. Thawornchaisit U, Pakulanon K (2007) Application of dried sewage sludge as phenol biosorbent. Bio Tech 98:140–144. DOI: 10.1016/j.biortech.2005.11.004
66. Trezza MA, Lavat AE (2001) Analysis of the system  $3\text{CaO}\cdot\text{Al}_2\text{O}_3 - \text{CaSO}_4\cdot 2\text{H}_2\text{O} - \text{CaCO}_3 - \text{H}_2\text{O}$  by FT-IR spectroscopy. Cement and Concrete Research 31:869–872. DOI: 10.1016/S0008-8846(01)00502-6. In: Awaleh MO, Farah IG, Adawe LF, Egueh NM, Soubaneh YD, Caminiti AM, Hoch FB, Etoubleau J (2014) Potentialite d'utilisation d'argiles Djiboutiennes dans l'industrie céramique. ScienceLib Editions Mersenne. 6, N°141106, ISSN 2111-4706
67. Uddin MT, Islam MS, Abedin MZ (2007) Adsorption of phenol from aqueous solution by water hyacinth ash. ARPN Journal of Engineering and Applied Sciences 2:11–17
68. Van der Marel HW, Beutelspacher H (1977) Atlas of infrared spectroscopy of clay Minerals and their admixtures

69. Wang X, Wang J, Zhang J (2012) Comparisons of Three Methods for Organic and Inorganic Carbon in Calcareous Soils of Northwestern China. PLOS ONE 7(8):e44334. <https://doi.org/10.1371/journal.pone.0044334>
70. Weber WJ, Morris JC (1963) Kinetics of adsorption on carbon from solution. Journal of the Sanitary Engineering Division American Society of Civil Engineers 89:31–60
71. Zidane F, Rhazzar A, Blais JF, Ayoubi K, Bensaid J, Basri EL, Kaba S, Fakhreddine N, et Lekhlif Q (2011) Contribution à la dépollution des eaux usées de textile par électrocoagulation et par adsorption sur des composés à base de fer et d'aluminium. Int Jiol Chem Sci 5:1727-1745. ISSN 1991-8631. DOI: 4314/ijbcs.v5j4.35

## Figures

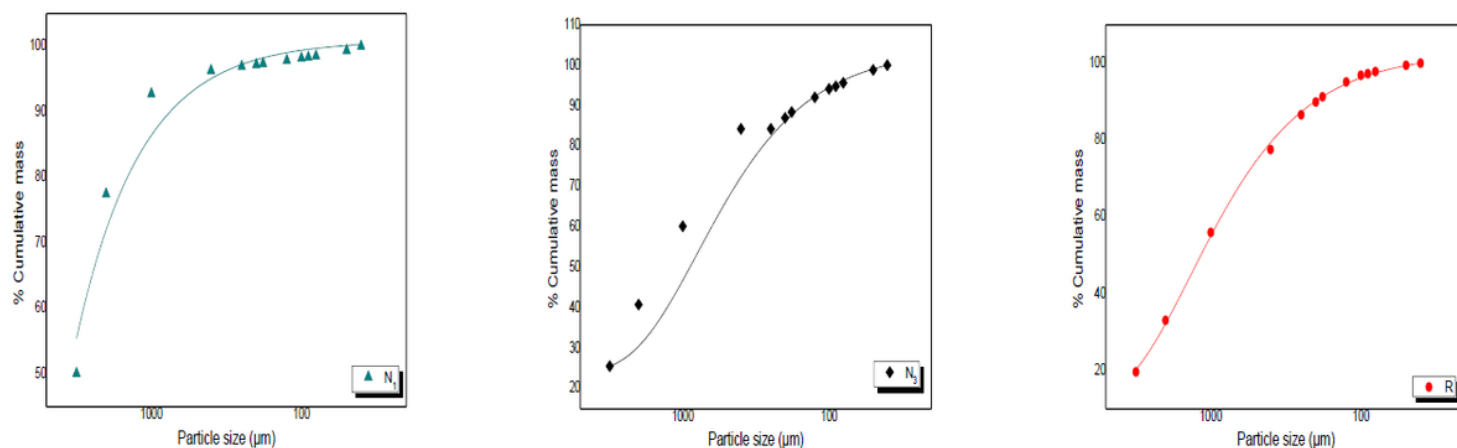


**Figure 1**

Particle size distribution of raw soils determined by sieving

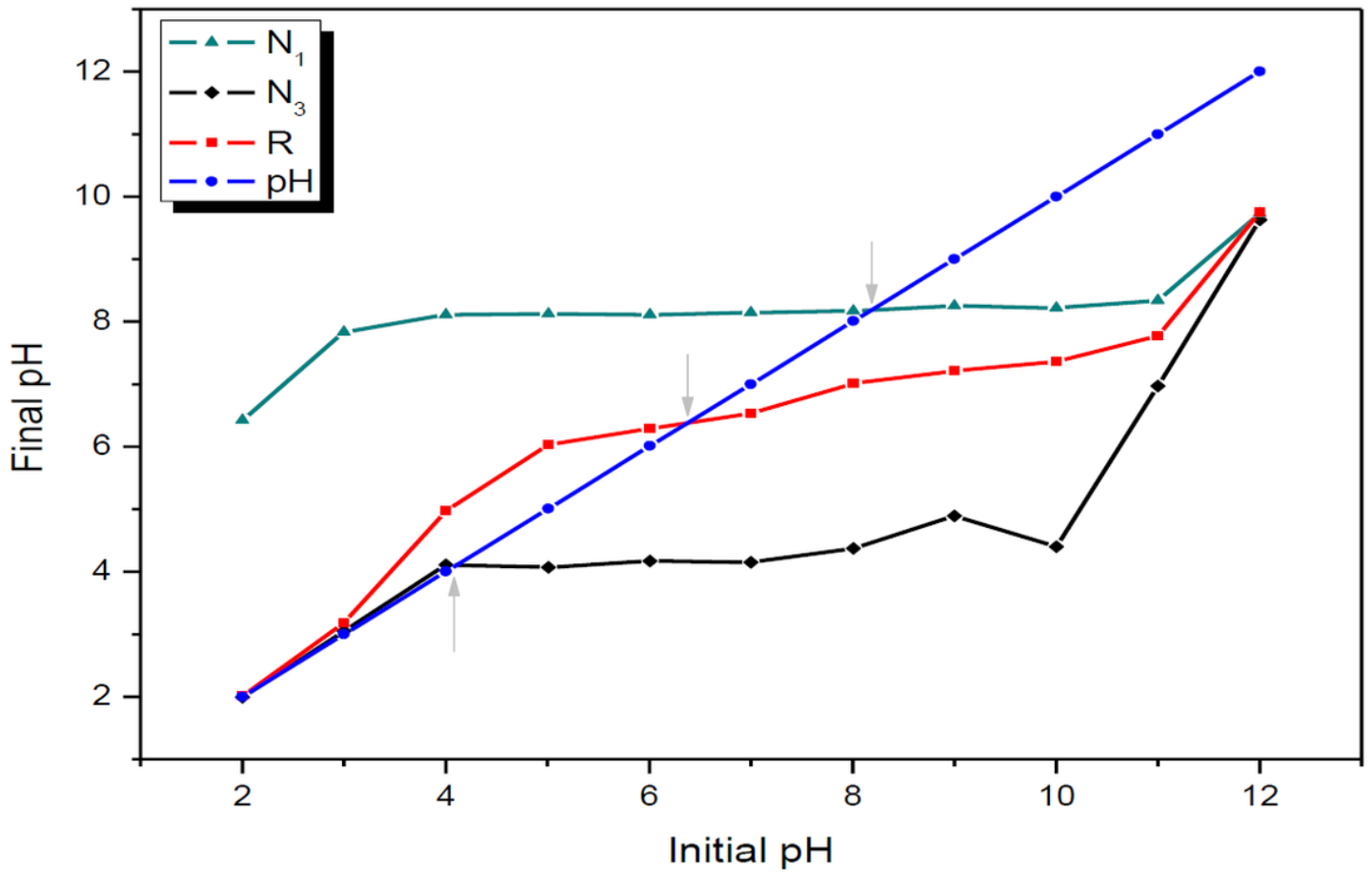
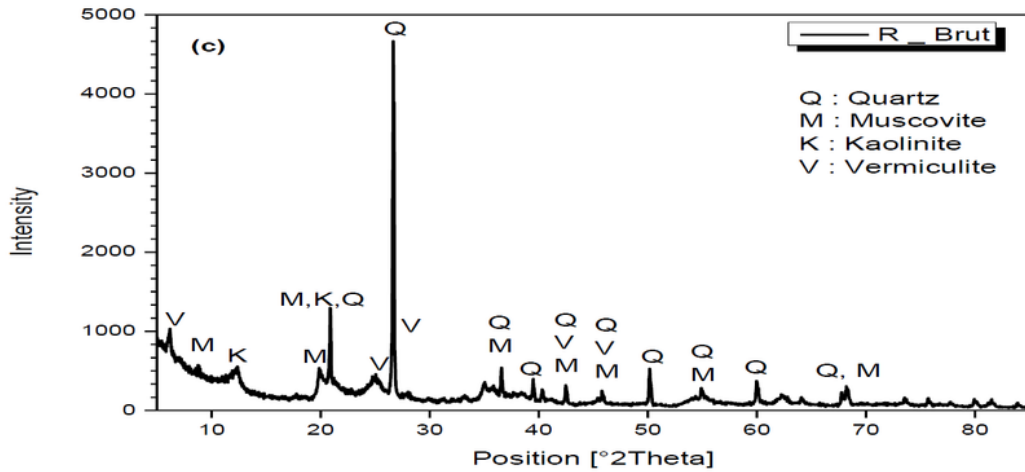
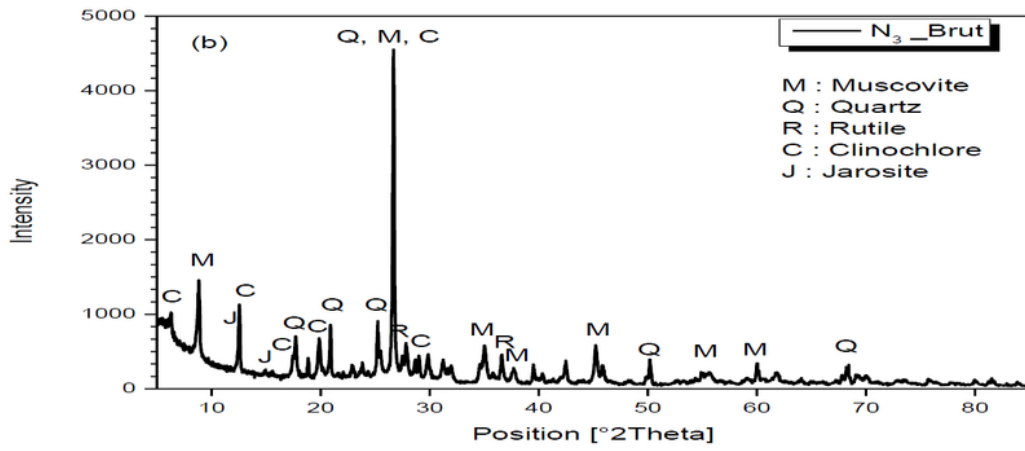
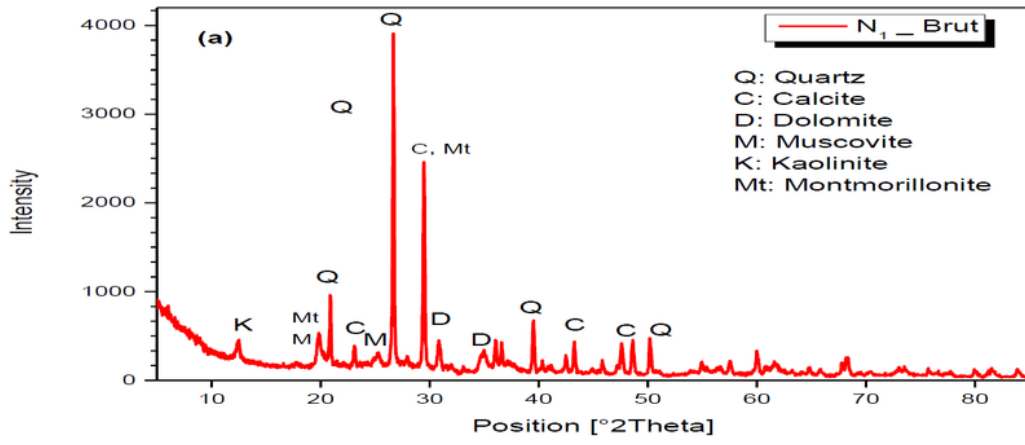


Figure 2

Curves: final pH = f (initial pH), the line : final pH = initial pH and the points pHzpc of the three soils



**Figure 3**

X-ray diffractograms of raw soils

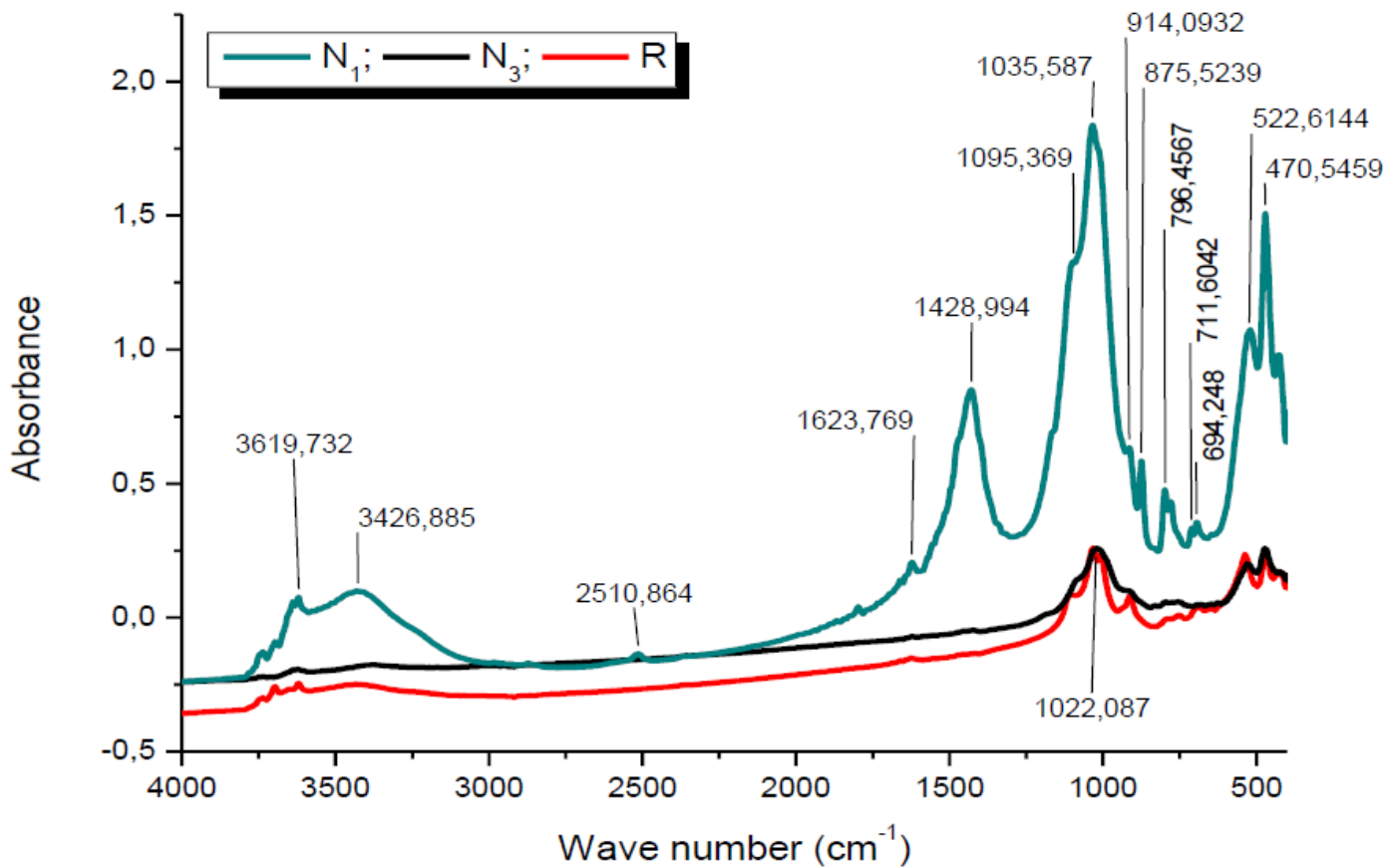


Figure 4

IRTF spectra of soils N1, N3 and R

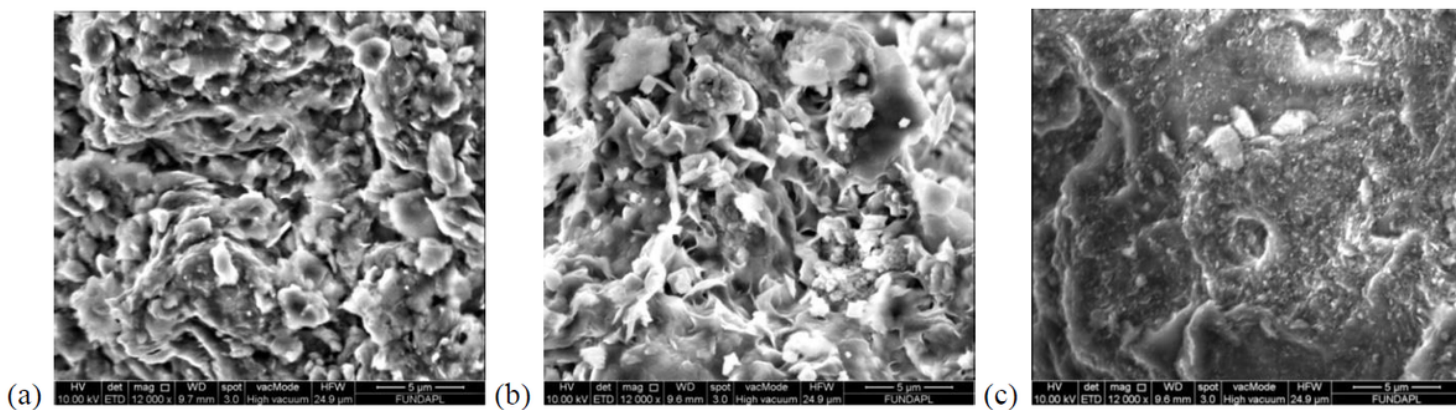


Figure 5

SEM micrographs of soils a N1, b N3 and c R

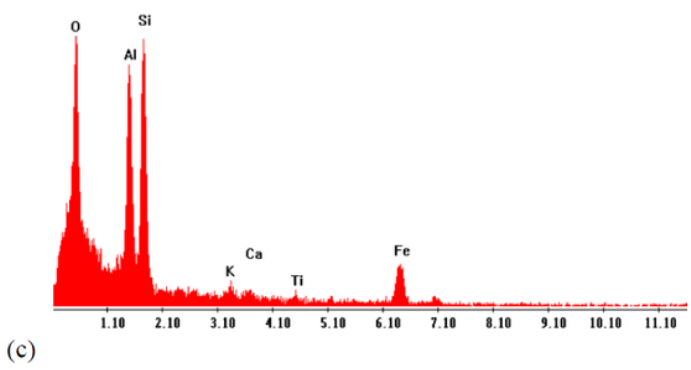
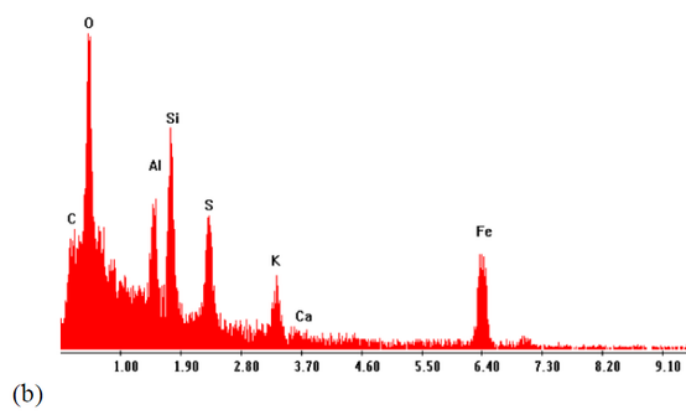
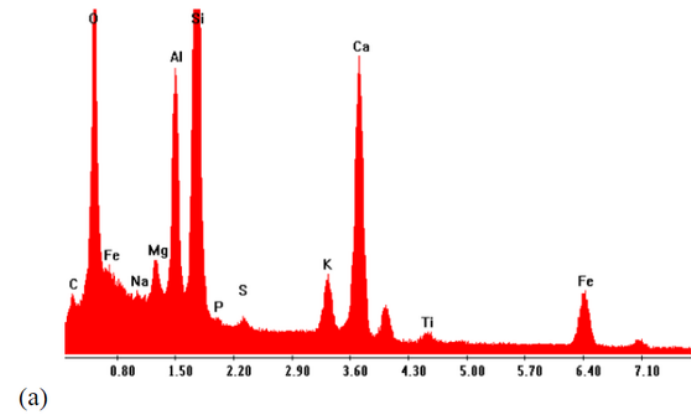
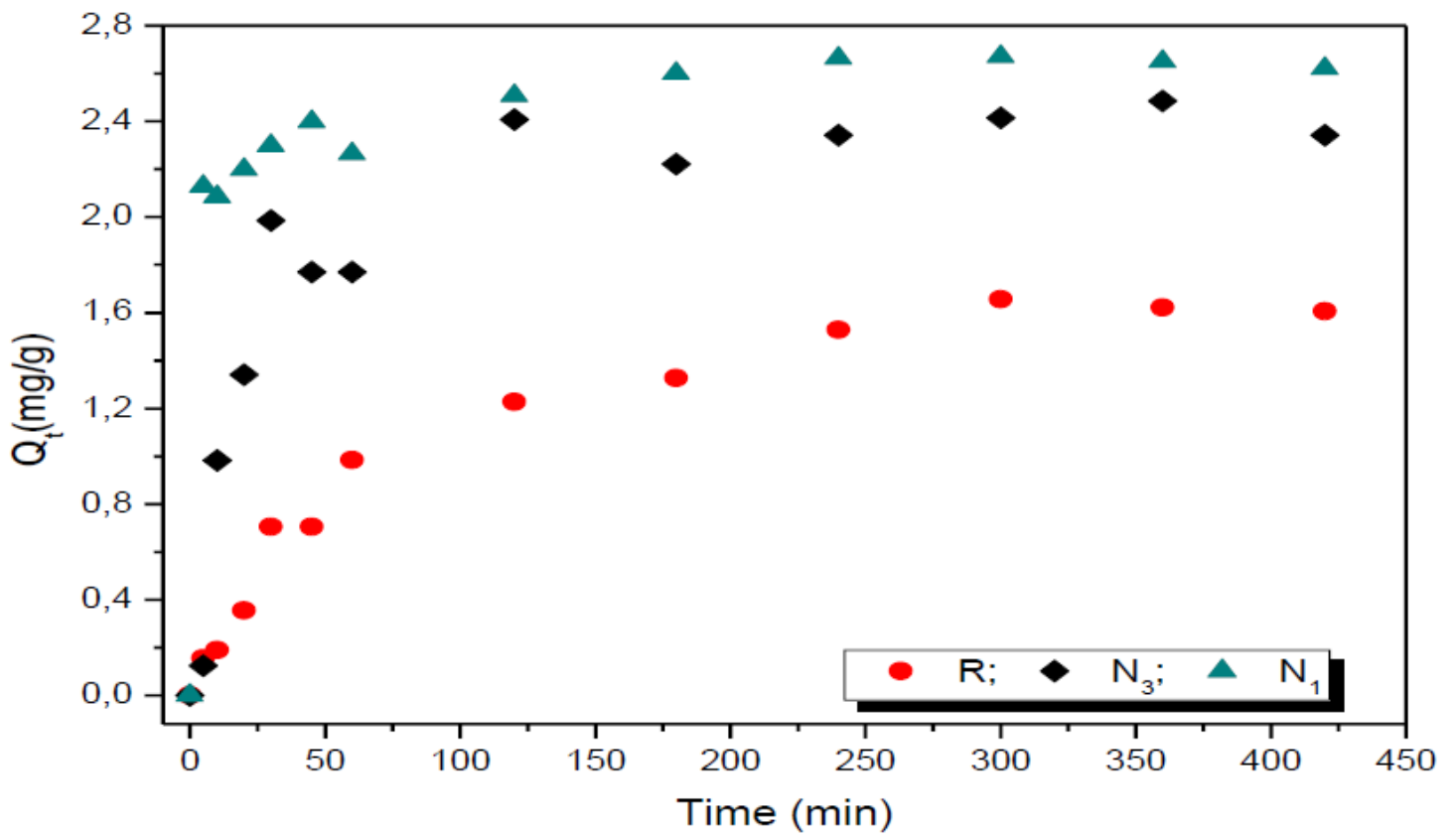


Figure 6

EDX analysis of soils a N1, b N3 and c R



**Figure 7**

Influence of contact time on the adsorption capacity of TPC ( $m = 2 \text{ g}$ ;  $\Phi = 400 \text{ }\mu\text{m}$ ;  $\text{pH}_{\text{effluent}} = 4.55$ ;  $[\text{TPC}] = 728 \text{ mg/L}$ ; Stirring speed = 250 rpm;  $v = 20 \text{ mL}$ ;  $T = 25 \text{ }^\circ\text{C}$ )

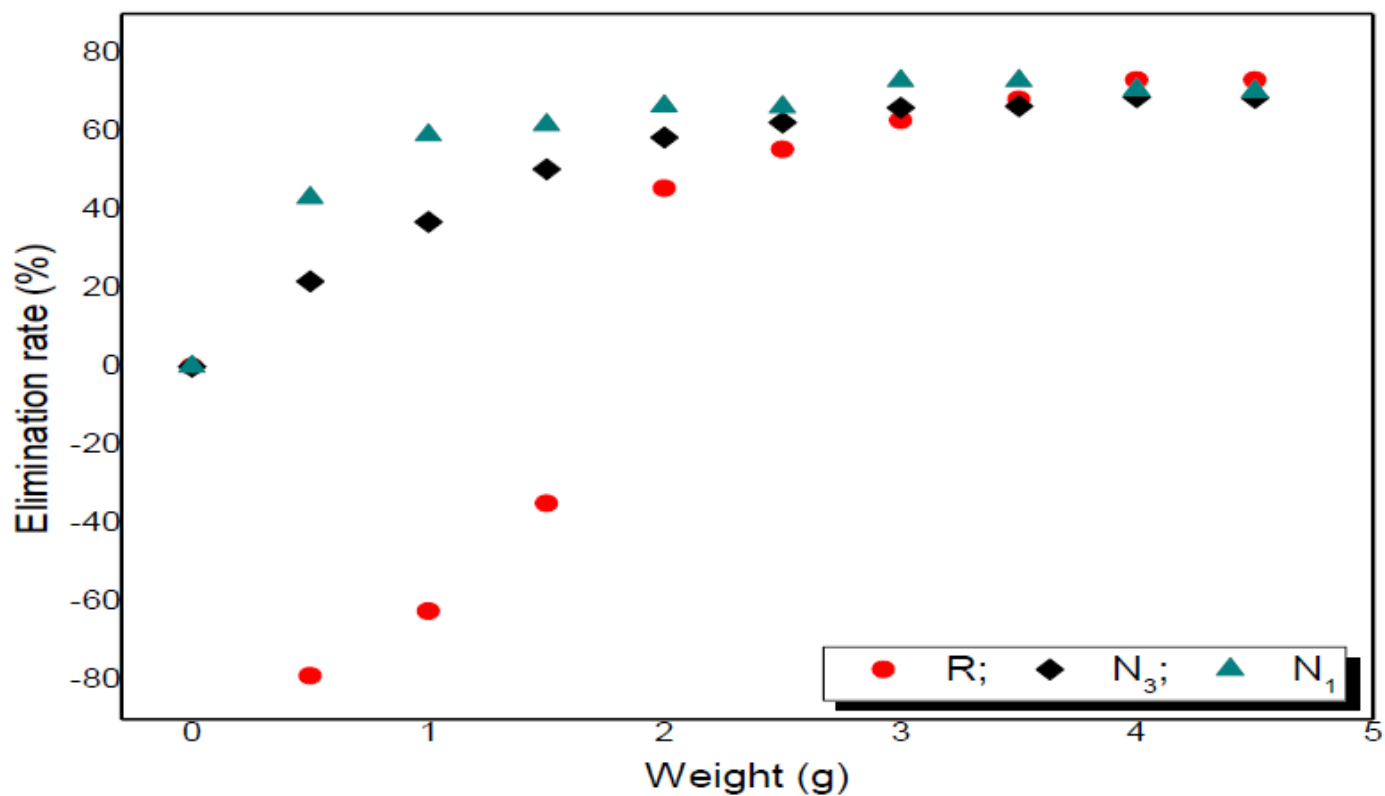
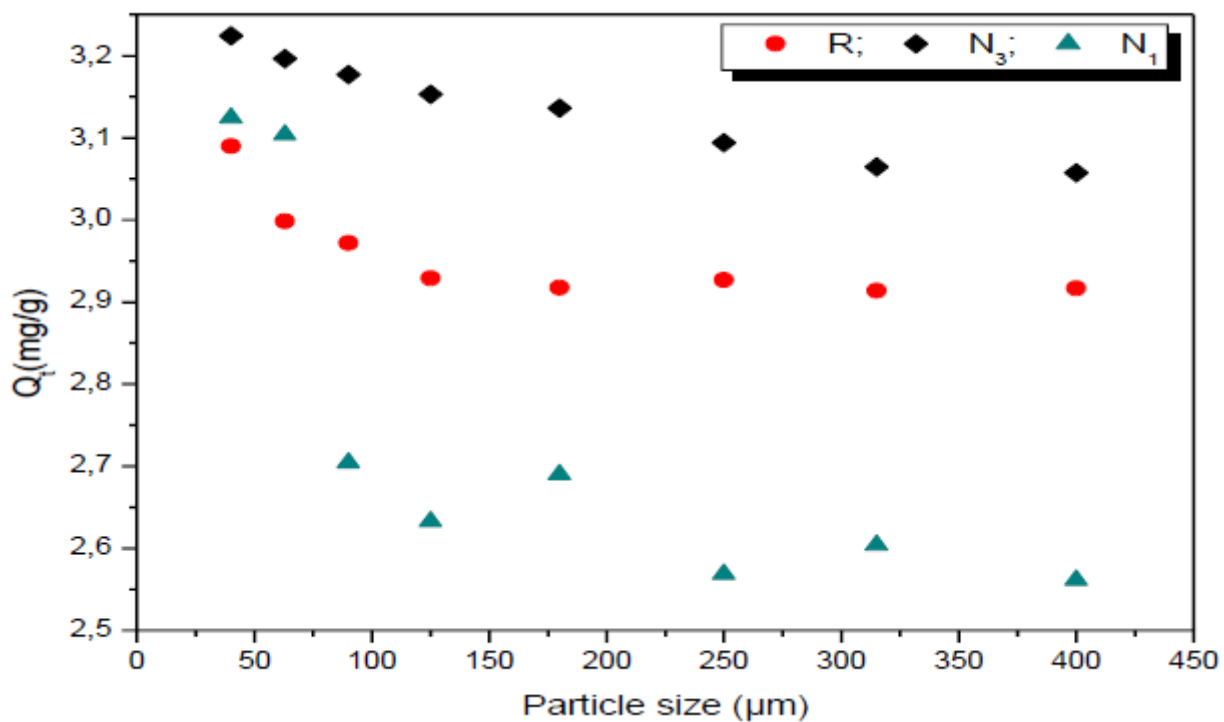


Figure 8

TPC removal rate as a function of the mass of the adsorbent ( $\Phi = 400 \mu\text{m}$ ;  $\text{pH}_{\text{effluent}} = 4.55$ ;  $[\text{TPC}] = 728 \text{ mg/L}$ ; Stirring speed = 250 rpm;  $v = 20 \text{ mL}$ ;  $T = 25 \text{ }^\circ\text{C}$ ;  $t = 24\text{h}$ )



**Figure 9**

Influence of particle size on the adsorption capacity of TPC ( $pH_{\text{effluent}} = 4.55$ ;  $[TPC] = 728 \text{ mg/L}$ ; Stirring speed = 250 rpm;  $v = 20 \text{ mL}$ ;  $T = 25 \text{ }^\circ\text{C}$ ;  $t = 24\text{h}$ ;  $m = 3.5\text{g}$ )

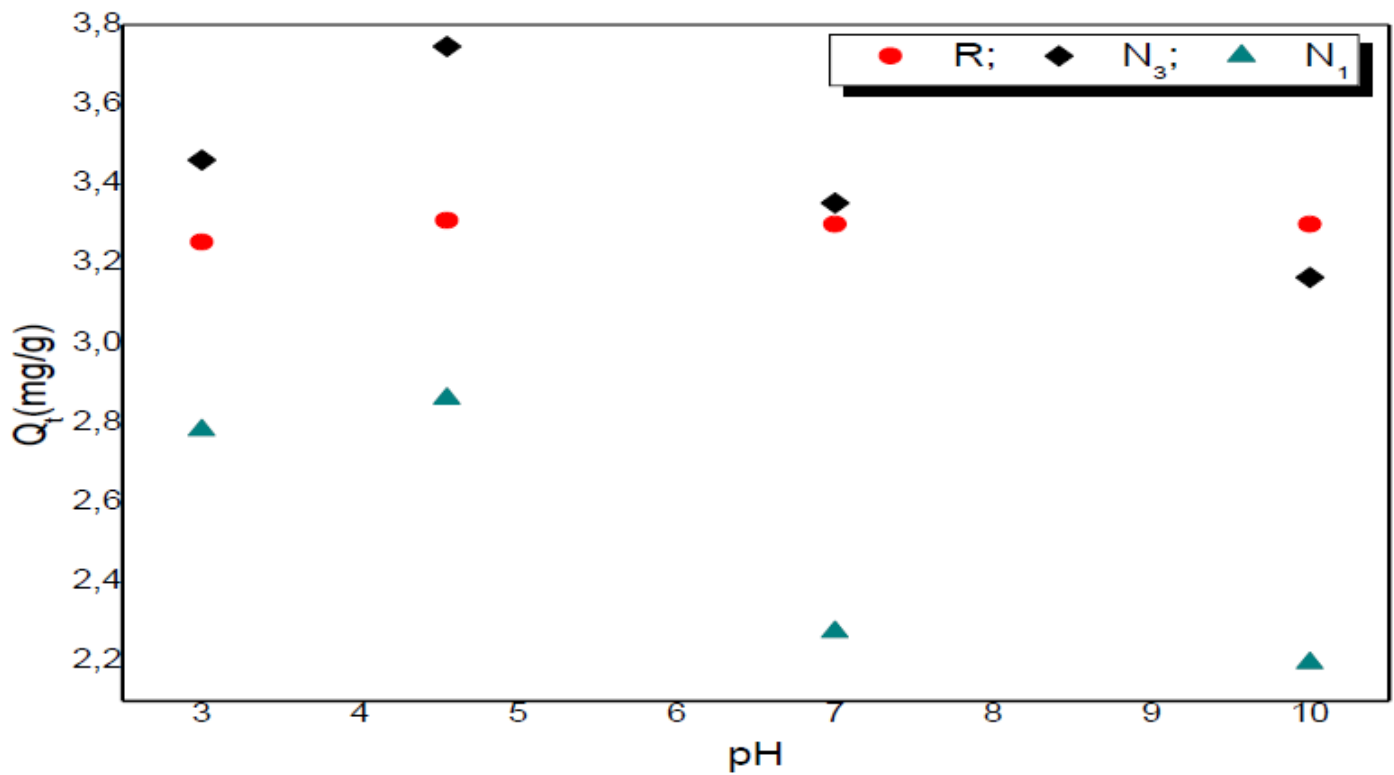


**Figure 10**

Influence of pH on the adsorption capacity of TPC ( $[TPC] = 728 \text{ mg/L}$ ; Stirring speed = 250 rpm;  $v = 20 \text{ mL}$ ;  $T = 25 \text{ }^\circ\text{C}$ ;  $t = 24\text{h}$ ;  $m = 3.5\text{g}$ ;  $\Phi = 40 \text{ }\mu\text{m}$ )

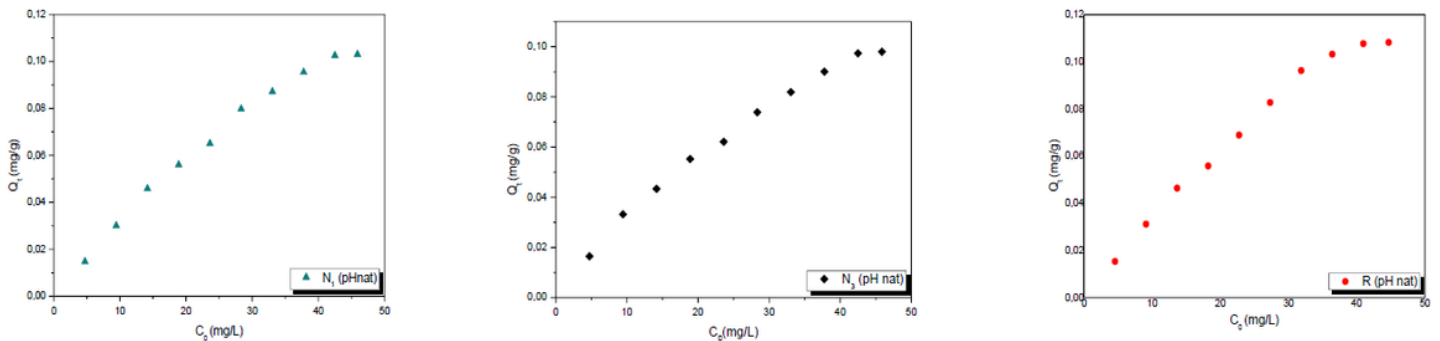


**Figure 11**

Influence of the initial TPC concentration (Stirring speed = 250 rpm;  $v = 20 \text{ mL}$ ;  $T = 25 \text{ }^\circ\text{C}$ ;  $t = 24\text{h}$ ;  $m = 3.5\text{g}$ ;  $\Phi = 40 \text{ }\mu\text{m}$ ;  $pH_{\text{effluent}} = 4.55$ )

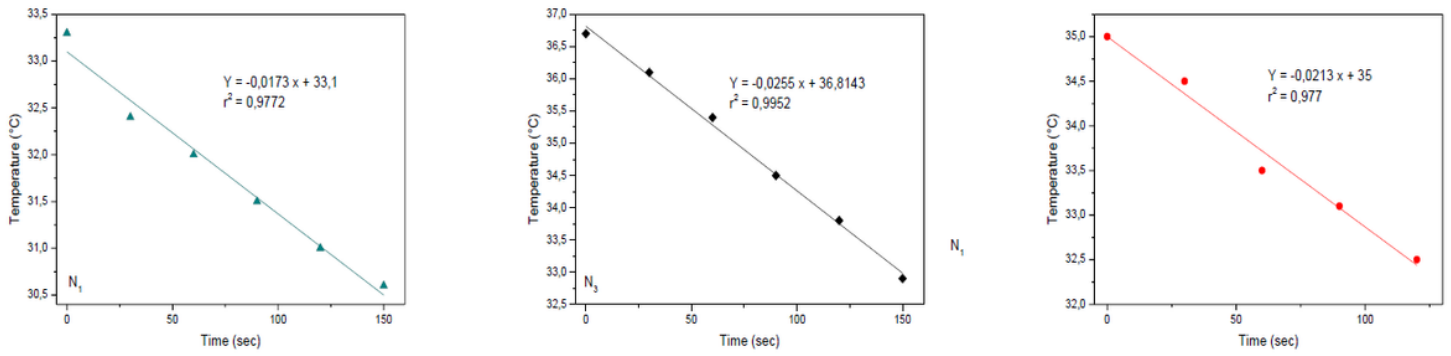


**Figure 12**

Temperature variation after microwave irradiation of natural soils a N<sub>1</sub>, b N<sub>3</sub> and c R (Stirring speed = 250 rpm; Power = 180 W; m = 3.5 g;  $\Phi$  = 180  $\mu$ m; t = 60 sec with steps of 5 sec; [TPC] = 663 ppm; v = 20 mL at pH = 4,55)

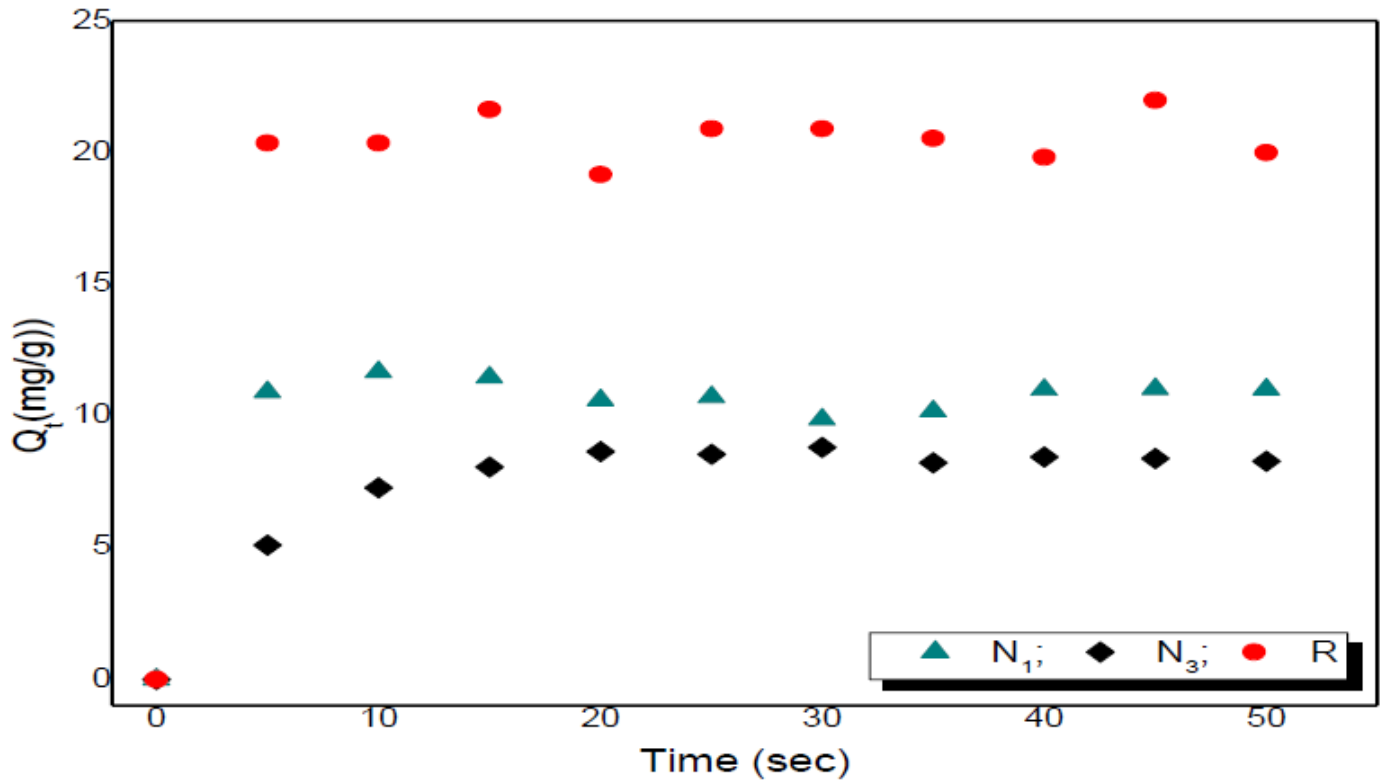
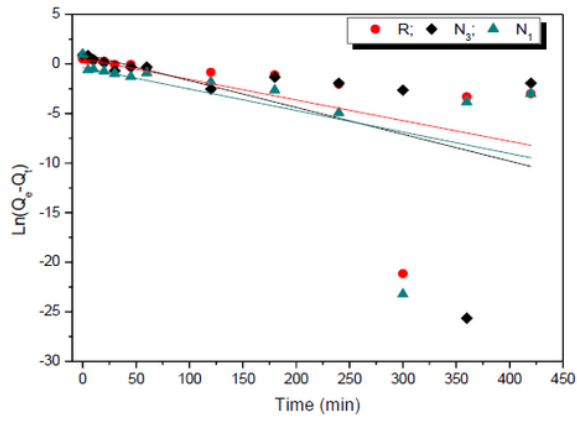
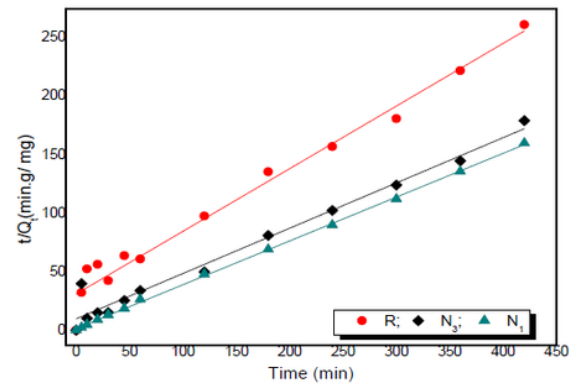


**Figure 13**

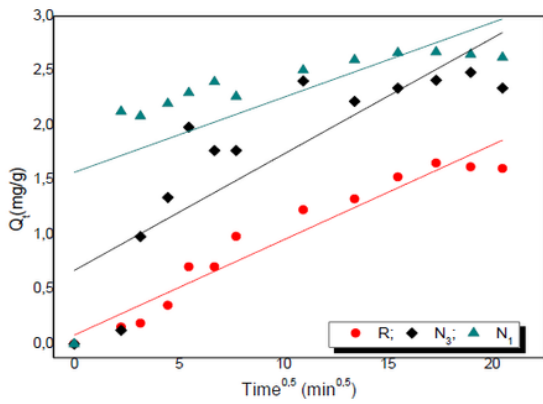
Influence of contact time on the adsorption of TPC under microwave activation (Stirring speed = 250 rpm; Power = 180 W; m = 3.5 g;  $\Phi$  = 180  $\mu$ m; [TPC] = 663 ppm; v = 20 mL; pH = 4.55; t = 60 with steps of 5 sec)



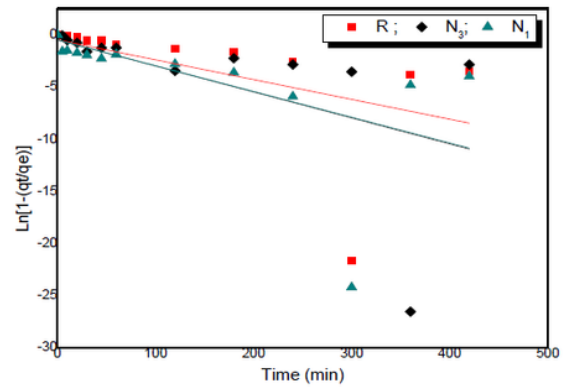
(a)



(b)



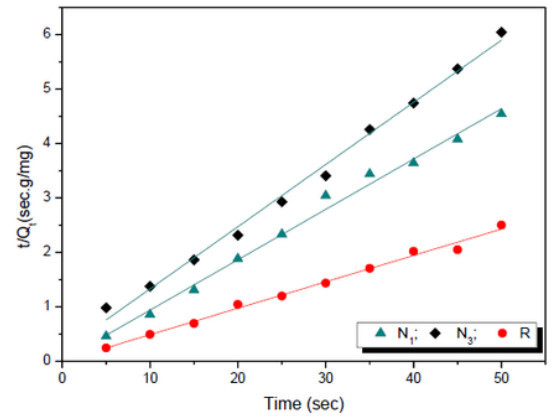
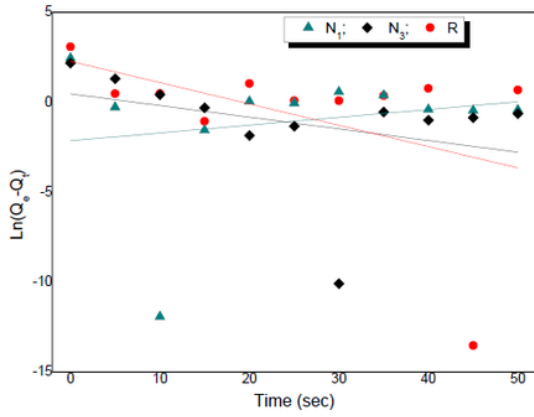
(c)



(d)

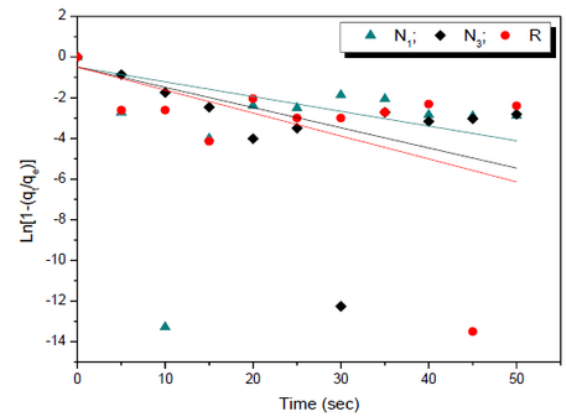
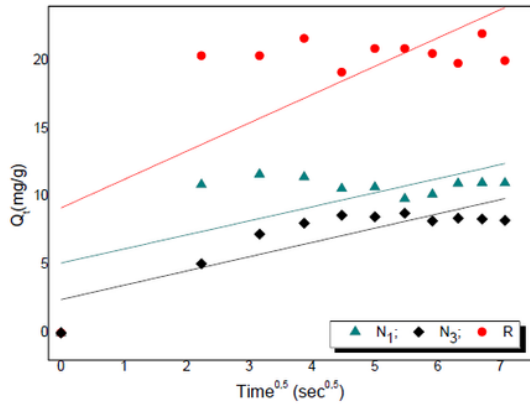
**Figure 14**

Kinetic linearization of the conventional adsorption of TPC on natural soils a pseudo-first order, b pseudo-second order, c intra-particle diffusion and d external diffusion



(a)

(b)



(c)

(d)

**Figure 15**

Kinetic linearization of adsorption under microwave activation of TPC on natural soils a pseudo-first order, b pseudo-second order, c intra-particle diffusion and d external diffusion

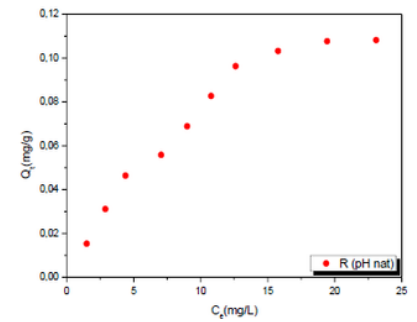
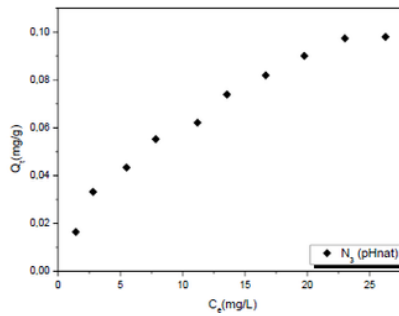
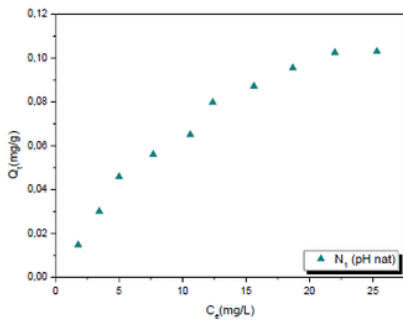


**Figure 16**

TPC adsorption isotherms (Stirring speed = 250 rpm; v = 20 mL; T = 25 °C; t = 24h; m = 3.5g;  $\Phi$  = 40  $\mu$ m; pH<sub>effluent</sub> = 4.55)

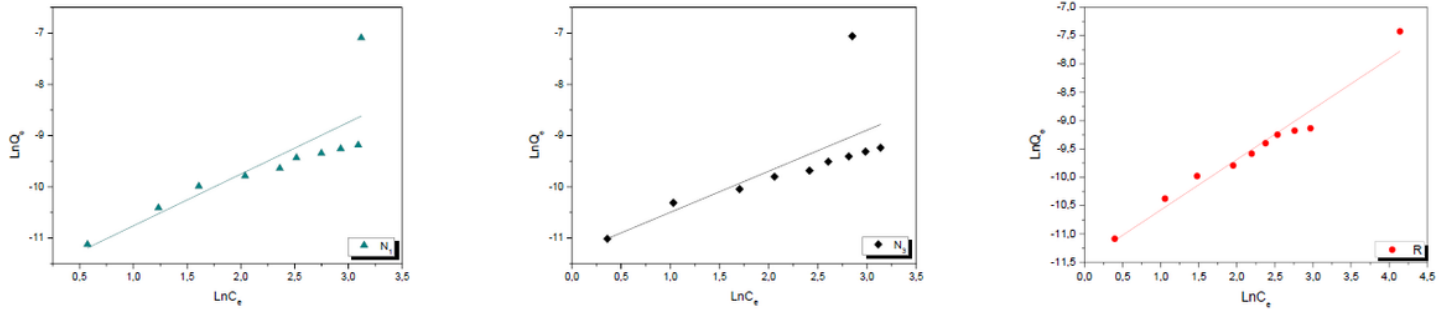


**Figure 17**

Linearization of the Freundlich isotherm for conventional sorption of TPC on N1, N3 and R soils at room temperature

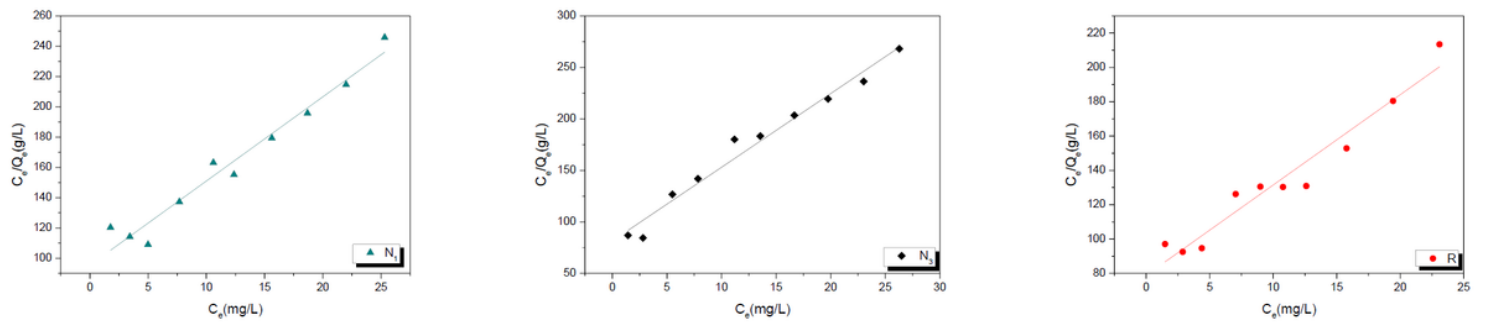


**Figure 18**

Linearization of the Langmuir isotherm for conventional sorption of TPC on N1, N3 and R soils at room temperature

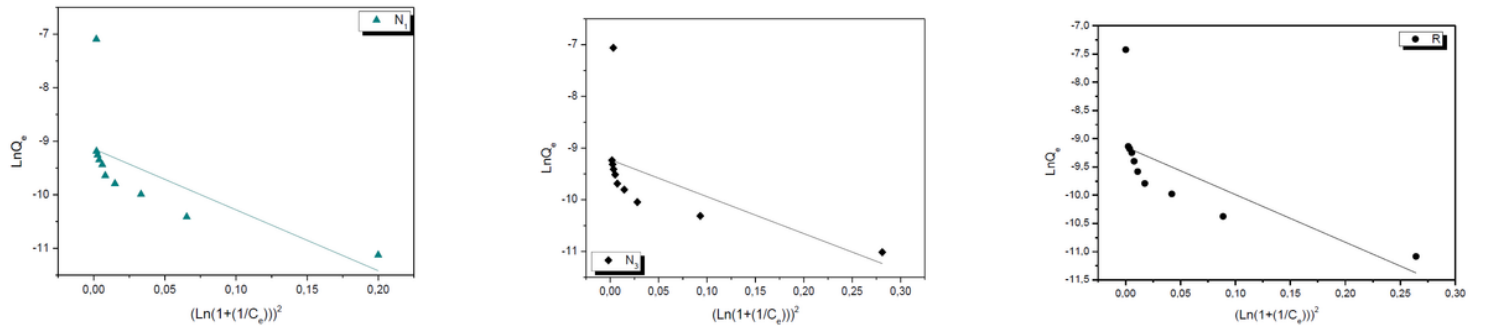


**Figure 19**

Linearization of the Dubinin-Radushkevich isotherm for conventional sorption of TPC on N1, N3 and R soils at room temperature